The Effect of Atmospheric Acid Processing on the Global Deposition of Bioavailable Phosphorus from Dust

R. J. Herbert[1, †] M. D. Krom[1, ‡] K. S. Carslaw[1], A. Stockdale[1], R. J. G. Mortimer[2], L. G. Benning[1, 3, 4], K. Pringle[1], J. Browse[1, *]

[1] School of Earth and Environment, University of Leeds, Leeds, LS2 9JT, UK.

[2] School of Animal, Rural and Environmental Sciences, Nottingham Trent University, Brackenhurst Campus, Southwell, Nottinghamshire, NG25 0QF, UK.

[3] GFZ German Research Centre for Geosciences, Telegrafenberg, 14473 Potsdam, Germany.

[4] Department of Earth Sciences, Free University of Berlin, 12249 Berlin, Germany.

Corresponding author: Ross Herbert (r.j.herbert@reading.ac.uk)

† Now at Department of Meteorology, University of Reading, Reading, RG6 6AH, UK.

‡ Now at Morris Kahn Marine Research Station, Department of Marine Biology, Leon H. Charney School of Marine Science, University of Haifa, Haifa, 3498838, Israel.

* Now at College of Life and Environmental Sciences, University of Exeter, Penryn, TR10 9EZ, UK.

Abstract

The role of dust as a source of bioavailable phosphorus (Bio-P) is quantified using a new parameterization for apatite dissolution in combination with global soil data maps and a global aerosol transport model. Mineral dust provides 31.2 Gg-P yr^{-1} of Bio-P to the oceans, with 14.3 Gg-P yr^{-1} from labile P present in the dust, and an additional 16.9 Gg-P yr^{-1} from acid dissolution of apatite in the atmosphere, representing an increase of 120%. The North Atlantic, northwest Pacific, and Mediterranean Sea are identified as important sites of Bio-P deposition from mineral dust. The acid dissolution process increases the fraction of total-P that is bioavailable from ~10% globally from the labile pool to 23% in the Atlantic Ocean, 45% in the Pacific Ocean, and 21% in the Indian Ocean, with an ocean global mean value of 22%. Strong seasonal variations, especially in the North Pacific, northwest Atlantic, and Indian Ocean, are driven by large-scale meteorology and pollution sources from industrial and biomass-burning regions. Globally constant values of total-P content and bioavailable fraction used previously do not capture the simulated variability. We find particular sensitivity to the representation of particle-to-particle variability of apatite, which supplies Bio-P through acid-dissolution, and calcium carbonate, which helps to buffer the dissolution process. A modest 10% external mixing results in an increase of Bio-P deposition by 18%. The total Bio-P calculated here (31.2 Gg-P yr^{-1}) represents a minimum compared to previous estimates due to the relatively low total-P in the global soil map used.

1 Introduction

Phosphorus (P) is an essential requirement for life. In the terrestrial ecosystem P is made accessible naturally through weathering processes and increasingly through the supply of fertilizer and other P-containing compounds from anthropogenic processes. The dominant supply of P to coastal systems is from rivers and wastewater discharge, which are augmented by sedimentary recycling processes (Ruttenberg, 2003). By contrast, in the offshore ocean the dominant external supply is from atmospheric deposition processes, with long-range transportation of mineral dust from desert regions being the most important single source of P to the ocean surface (Graham and Duce, 1982; Mahowald et al., 2008; Myriokefalitakis et al., 2016). In-situ measurements of atmospheric aerosol (e.g., Carbo et al., 2005; Herut et al., 1999; Zamora et al., 2013) and soil mineralogical databases (Nickovic et al., 2012; Yang et al., 2013) show that total P (hereafter TP) content of soils and mineral dust is spatially and temporally variable and may range from < 500 to > 1000 ppm, with corresponding variability in the component P pools.

Many studies show the importance of atmospheric supply in general and dust in particular as a source of external nutrients (Fe, N and P) to the open ocean (Krishnamurthy et al., 2010; Mahowald et al., 2008). In such systems, the total N supplied is in a readily bioavailable form. In contrast the P (and Fe) is supplied in both labile (and hence bioavailable) and non-bioavailable forms. The non-bioavailable particles of P can drop through the photic zone without enhancing phytoplankton growth and hence carbon uptake. Herut et al. (2005) showed that when fresh Saharan dust and dust pre-treated to remove any water-leachable nutrients were added to a microcosm experiment containing N- and P-limited Mediterranean seawater only the fresh dust resulted in increased chlorophyll content. The fresh dust added nutrients in the ratio of 31N:1P (nitrate:phosphate) and thus it was the water-leachable fraction of the dust rather than the particle itself that caused the extra productivity in this N and P co-limited system (Thingstad et al., 2005). Eijsink et al. (2000) found that even in the P-limited Eastern Mediterranean, 70% of the TP (mainly detrital apatite) supplied as Saharan dust to the surface waters was transferred through the water column and ended up deposited in the sediment. The remaining 30% was taken up by biological processes in the water column.

Observations suggest that the percentage of TP in mineral dust that is deposited in a bioavailable form (Bio-P) is spatially variable, ranging from < 10% to > 80% (Baker et al., 2006a; Markaki et al., 2003; Zamora et al., 2013; Vet et al., 2014), and may increase with distance from the dust source (Baker et al., 2006a). Recent ambient observations and laboratory experiments (Nenes et al., 2011; Srinivas and Sarin, 2015; Stockdale et al., 2016) provide support for the hypothesis that atmospheric acidification and subsequent dissolution is a primary process for producing Bio-P in mineral dust. Increasing the amount of leachable, or bioavailable, P by acid processes in the atmosphere will have a direct effect of increasing phytoplankton biomass and hence carbon uptake in a variety of ocean systems (e.g., Jickells and Moore, 2015; Mahowald et al., 2008)

The paucity of observational data from the open oceans necessitates the use of models to determine the atmospheric flux of Bio-P to surface waters. Models are also needed to quantify how Bio-P deposition may change with environmental factors such as source strength, atmospheric pollution, and large-scale changes to global circulation. To achieve this, models must represent the emission, transport and deposition of the particulate P, as well as processes

that determine the TP and Bio-P content. Previous global deposition modelling studies using global chemical transport models (Brahney et al., 2015; Krishnamurthy et al., 2010; Mahowald et al., 2008; Wang et al., 2015) assumed that dust emissions contain a constant fraction of TP (between ~720 and 1050 ppm) and a constant percentage of TP deemed Bio-P (between 10% and 15%). The result is a spatially varying flux of dust-borne P to the surface with a constant solubility, which may not reflect underlying variability between dust sources, nor atmospheric acidification processes. A recent study by Myriokefalitakis et al. (2016) represented the acidification process using an acid-solubilization mechanism in which apatite dissolution is treated as a kinetic process dependent on the H^+ activity of the surrounding water droplet and known acid dissolution thermodynamic constants. Their study used a global soil mineralogy dataset (Nickovic et al., 2012) to represent the spatially varying soil TP content with dust-TP emissions adjusted to a global mean of 880 ppm and a soluble fraction of 10% representing a leachable inorganic pool of P in the initial dust. The remaining TP was assumed to be apatite. This treatment reproduces the atmospheric acidification process but relies on several assumptions for estimating the different forms of P. A recent global soil database (Yang et al., 2013) provides high resolution information on the geographical distribution of TP in its different forms including apatite, labile, organic, occluded, and secondary P. The dataset shows that there is considerable spatial variability in all components. This dataset provides more appropriate forms of P for use in estimating dust-borne P emissions and simulating atmospheric acidification processes of apatite.

A recent study by Stockdale et al. (2016) presents results from a series of experiments simulating atmospheric acidification on dust samples and dust precursor soils in which the acidity of the solution and the mass of dust was systematically varied. Phosphorus speciation experiments identified the dominant forms of phosphorus in the dust samples as ~80% apatite P, ~10% Fe-bound P, and ~10% labile-P. The acidification experiments provide robust evidence for a relatively simple relationship in which the dissolution behaviour of mineral dust is controlled by the absolute number of protons in the solution, the calcium carbonate ($CaCO_3$) content, and the apatite (Ap-P) content of the dust. Rapid acid dissolution of both mineral species occurs simultaneously when both minerals are present on the same mineral grain (internally mixed). The dissolution rate of Ap-P is greater when the Ap-P and $CaCO_3$ exist on different grains (externally mixed). As a result of slow mineral precipitation kinetics the dissolved phosphate remains in solution when the H^+ concentration falls or water content increases. The total mass of Bio-P upon deposition to the surface is thus the sum of acid-dissolved apatite (Acid-P) and the loosely bound labile P (Lab-P) that was initially available in the particles. As the dissolution of Ap-P occurs at a faster rate when $CaCO_3$ is not present, if Ap-P and $CaCO_3$ where exclusively present on different particles (i.e., externally mixed) then it is possible that more Acid-P would be produced. As discussed by Stockdale et al. (2016) it is hypothesized that many particles would contain both Ap-P and $CaCO_3$, however, there is likely a degree of variation between particles with some containing more or less of each mineral component.

It is widely recognized that mineral dust plays an important role in the transport of nutrients to the open ocean surfaces, however, as shown by Yang et al. (2013) there exists considerable variability in the relative abundance of different P-containing components from different source regions. The results of Stockdale et al. (2016) additionally show that the spatial distribution of $CaCO_3$ and its abundance in relation to Ap-P may have considerable impacts on the production

of Bio-P from acid dissolution of Ap-P. The simplistic dissolution mechanism presented by Stockdale et al. (2016) and the detailed soil-P speciation dataset presented by Yang et al. (2013) provide a new and readily applicable method for estimating the spatio-temporal distribution of Bio-P from dust and allows us to investigate the sensitivity of Acid-P production to the degree of internal and external mixing of the components. This will help to understand key uncertainties in the acid dissolution process and help better define the focus of future research.

In this study we use the Global Model of Aerosol Processes (GLOMAP) coupled to the global chemical transport model TOMCAT to simulate the emission, transport, and deposition of dust-borne phosphorus to the surface. Apatite dissolution parameterizations based on the results from Stockdale et al. (2016) and a database of soil P speciation (Yang et al., 2013) are used to simulate atmospheric acidification of mineral dust by H_2SO_4 and HNO_3; the soil database is also used to simulate the contribution of the dust-borne Lab-P as a spatially variable percentage of dust mass. These results are used to investigate the drivers of the spatio-temporal variability in dust-borne Bio-P and the Acid-P (the amount of TP converted to Bio-P by atmospheric acid processes). The results are compared to a global dataset of observations (Vet et al., 2014) and results from other modelling studies to help understand the importance of atmospheric acidification of mineral dust on the global supply of P nutrients to the open oceans and elsewhere. Finally, simulations are performed to investigate the sensitivity of the results to the effect of external mixing of apatite and $CaCO_3$ on the amount of Bio-P delivered to the ocean surface.

2 Model description

We use the global aerosol microphysics model GLOMAP-mode (Mann et al., 2010) coupled to the 3D global chemical transport model TOMCAT (Chipperfield, 2006). Simulations are performed using a horizontal resolution of 2.8° by 2.8° and 31 hybrid σ-pressure levels extending from the surface to 10 hPa. Meteorology for the simulated year is driven by the European Centre for Medium-Range Weather Forecasts (ECMWF) ERA-Interim reanalyses at 6-hourly intervals Monthly mean low-cloud fields are prescribed from the International Satellite Cloud Climatology Project (ISCCP) archive. In the standard GLOMAP-mode setup the aerosol particle number and size distribution is described using a modal scheme with 7 internally mixed modes (4 soluble and 3 insoluble) and 5 aerosol species: sulfate, black carbon, organic carbon, sea-salt, and dust. The 7 modes cover four size ranges: nucleation (~1 to 10 nm diameter), Aitken (~10 to 100 nm), accumulation (~0.1 to 0.5 μm), and coarse (~0.5 to 10 μm).

The aerosol processes treated in the model include primary and precursor emissions, nucleation of H_2SO_4 aerosol, sedimentation and dry deposition, hygroscopic growth, in-cloud activation and scavenging, below-cloud scavenging, inter- and intra-modal coagulation, condensation of H_2SO_4 and secondary organic vapors onto all aerosol particles, ageing of water-insoluble particles, and in-cloud processing (formation of sulfate mass from oxidation of sulfur dioxide in aerosol particles activated into cloud droplets). GLOMAP-mode also includes an aerosol precursor chemistry scheme primarily for simulating gas and aqueous phase reactions leading to the production of SO_2 and H_2SO_4.

Monthly emissions of anthropogenic BC, OC, and SO_2, and volcanic SO_2 are supplied by global datasets from AeroCom hindcast (Diehl et al., 2012). The Global Fire Emissions Database (GFED) v2 database (van der Werf et al., 2010) is used for wildfire emissions, and dimethyl sulfide (DMS) emissions are calculated using DMS seawater concentrations from Kettle et al. (1999) and transfer velocity parameterizations of Nightingale et al. (2000). Daily size-resolved emissions of dust (covering accumulation and coarse modes) are included via prescribed fluxes from AeroCom (Dentener et al., 2006). Deposition of aerosol species occurs via dry deposition, using a dry deposition velocity following Slinn (1982), and wet deposition through nucleation scavenging from large-scale and convective precipitation (activation of cloud condensation nuclei), impaction scavenging by precipitation, and scavenging by low-cloud drizzle (Browse et al., 2012). The aqueous chemistry scheme includes the dissolution of SO_2, H_2O_2, and O_3 into cloud droplets and the subsequent oxidation of S(IV) to S(VI) by H_2O_2 and O_3. Condensation of H_2SO_4 onto aerosols is simulated using coefficients following Fuchs and Sutugin (1971) with added correction factors for molecular effects and limiting interfacial mass transport, the latter using an accommodation coefficient 1.0 for both insoluble and soluble modes as per Mann et al. (2010). For this study, the condensation of HNO_3 onto dust has been added following the above method; HNO_3 concentrations are taken from the coupled TOMCAT model with condensation acting as a sink to the HNO_3 fields. For simplicity, the condensed HNO_3 is added to the sulfate component as an equivalent mass of H_2SO_4 that would produce the same mass of H^+ ions upon dissociation of HNO_3.

In this study we are interested in the sulfate associated with dust aerosol, rather than the sulfate associated with sea-salt, and thus have altered the model setup to isolate the dust-associated sulfate which will be used to determine the amount of associated acid. Full details can be found in the supporting information (Text S1). The resulting annual dust deposition flux, shown alongside the data from the standard setup, is compared to AeroCom observations (Huneeus et al., 2011) in the supporting information (Figure S1) and shows the current setup is able to simulate dust deposition fluxes both close to source and in remote regions and is comparable to the original GLOMAP setup.

To simulate the acid dissolution process in GLOMAP two soil databases were used to provide information on the dust mineralogy. For the different forms of P in the dust the soil phosphorus database presented by Yang et al. (2013) was used. The database uses a global distribution of soil parent material and lithological dependent P concentrations along with a pedogenesis transformation model to simulate the weathering of each parent rock type. The authors present global distributions of P in different forms as an average of the top 50 cm of the soil profile, including total-P (TP), labile inorganic P (Lab-P), and apatite-P (Ap-P). A database of global soil $CaCO_3$ content was obtained from the gridded Global Soil Dataset for use in Earth System Models (GSDE) developed by Shangguan et al. (2014). A mean content was determined using the top 50cm of data in order to provide comparable emissions to the P components and to maximise global coverage of emissions. Figure 1 shows the datasets regridded to a 2.8° horizontal resolution. Dust TP content typically ranges from 200 – 1000 ppm by mass (global mean of 563 ppm), Ap-P from 20 – 300 ppm (164 ppm), and Lab-P from 20 – 100 ppm (50 ppm), whilst $CaCO_3$ content, at over two orders of magnitude greater, typically ranges from 1 – 12% (global mean of 3.3%) of the total dust mass. In terms of global means Lab-P constitutes 9% of TP dust content and varies between 5 – 10%, whereas Ap-P constitutes 29% of TP and

varies between 5 – 60%; the major deserts show less variability and Ap-P tends to represent ~50% of TP. The form of P that represents the majority of remaining TP is occluded-P (not shown; spatial distribution apparent from the low values of Ap-P:TP). Experimental observations from Stockdale et al. (2016) suggest this form of P is not released through acid dissolution nor upon deposition to the ocean surface; it is also much more prevalent in the northern boreal regions where dust uplift is less important.

To simulate the emission and deposition of the dust mineralogy, tracers were included in GLOMAP alongside dust following previous studies (Atkinson et al., 2013 and Vergara-Temprado et al., 2017) using the regridded soil-P and $CaCO_3$ datasets. For each tracer the spatially variable mass fraction of the components from the regridded soil-P and $CaCO_3$ databases were applied to the modelled dust emission at each grid point to produce an associated mass. Throughout the simulation, dust is considered a single component with the fractional partition between the constituents conserved for all processes, including interaction between two dust modes. The simulations produce monthly mean wet and dry mass deposition fluxes (both impaction and nucleation scavenging) from each grid point for total dust, TP, Ap-P, Lab-P, $CaCO_3$, and dust-associated acid in the form of the sulfate component.

The acid dissolution process is simulated using parameterizations based on experimental observations from Stockdale et al. (2016), which provide robust evidence that the dissolution of Ap-P occurs rapidly (seconds to minutes) and that the system can be replicated by a simple liner relationship between acid input and Ap-P / $CaCO_3$ dissolution. Linear fits to the experimental data on a logarithmic scale using all dust samples provides the mass of dissolved Ap-P and $CaCO_3$ as a function of the absolute number of protons available. The dissolution rate of Ap-P increases in the absence of $CaCO_3$, therefore an additional step has been introduced to simulate the enhanced dissolution rate. Stockdale et al. (2016) found that the dissolution of hydroxyapatite powder was well reproduced by the geochemical PHREEQC model (Parkhurst and Appelo, 2013); this model was used to produce a linear fit between available protons and dissolution of Ap-P, which provides a means for estimating Ap-P dissolution in the absence of $CaCO_3$. The resulting parameters from the linear fits can be found in the supporting information (Table S1). At each grid point (horizontal and vertical) the number of protons available, determined from the mass of dust-associated sulfate and assuming each mole of H_2SO_4 dissociates to produce 2 moles of H^+, is used to determine the number of moles of deposited dissolved $CaCO_3$ ($\mathrm{mol\ CaCO_{3_{diss}}}$) using Eq. 1. Applying $\mathrm{mol\ CaCO_{3_{diss}}}$ to Eq. 2 provides dissolved Ap-P ($\mathrm{mol\ Ap\text{-}P_{diss}}$) from simultaneous dissolution of Ap-P and $CaCO_3$. If all $CaCO_3$ has been dissolved (i.e., $\mathrm{mol\ CaCO_{3_{diss}}} = \mathrm{mol\ CaCO_{3_{available}}}$) any excess protons are used to determine a second source of $\mathrm{mol\ Ap\text{-}P_{diss}}$ using Eq. 2 under the condition that $\mathrm{mol\ CaCO_{3_{available}}} = 0$. The number of moles of dissolved Ap-P from simultaneous and separate dissolution, constrained by the available deposited mass of Ap-P, is integrated over each horizontal grid point to provide a monthly mean surface deposition flux of bioavailable P from Ap-P dissolution. The deposition fluxes of Lab-P are similarly integrated over each grid point and added to the dissolved Ap-P to provide the total atmospheric bioavailable P flux to the surface from inorganic mineral dust.

$$\log_{10}\left(\mathrm{mol\ CaCO_{3_{diss}}}\right) = a1 + b1 \cdot \log_{10}(\mathrm{mol\ H^+}) \quad (1)$$

$$\log_{10}(\text{mol Ap-P}_{\text{diss}}) = \begin{cases} a2 + b2 \cdot \log_{10}(\text{mol CaCO}_{3\,\text{diss}}), & \text{if mol CaCO}_{3\,\text{available}} > 0 \\ a3 + b3 \cdot \log_{10}(\text{mol H}^{+}_{\text{excess}}), & \text{if mol CaCO}_{3\,\text{available}} = 0 \end{cases} \quad (2)$$

3 Results

3.1 Bioavailable phosphorus

Annual deposition fluxes of bioavailable phosphorus (Bio-P) from dust, dust mass, and the dust-associated acid for the year 2001 are shown in Figure 2. The large spatial variability in dust deposition drives the spatial variability of Bio-P. Highest values are found close to major dust source regions of Sahara and Kalahari deserts in Africa, and across central Asia, the Americas, and Australia. A significant proportion of the dust is deposited close to the source of emission. However, considerable transport occurs from all dust source regions driven by large-scale meteorology, most notably the transport of African dust advecting westwards across the Atlantic Ocean driven by trade winds, and mid-latitude transport from South America and South Africa eastwards. Northern Hemisphere mid-latitude transport from Asia across the western and central Pacific Ocean also provides a considerable transport route for dust to these remote ocean regions. The amount of acid condensed onto the mineral dust (Figure 2c) shows a strong correlation with regions of high pollution and dust transport. The industrialized regions of North America, Europe, central and eastern Asia can be clearly identified, as well as regions of biomass burning in central Africa. Transported pollutants also play a considerable role over the north-west Pacific and North Atlantic, as well as northern Africa and the Mediterranean Sea. The low dust loading in the central Pacific and Atlantic coincident with a moderate amount of acid highlights the marine source of sulfate emissions from DMS in this region, and a similar correlation in the northern high latitudes highlights the transport of pollutants from Europe and North America to this remote region.

Table 1 provides a breakdown of absolute mass and mass per unit area deposited per year globally, on terrestrial ecosystems, on marine ecosystems, and into each ocean basin and continent; boundaries to each basin are shown in the supporting information (Figure S2). Globally, 117 Gg-P yr^{-1} Bio-P from mineral dust is deposited to the surface annually, with 86 Gg-P yr^{-1} to the continents and 31 Gg-P yr^{-1} to the oceans and seas. The large value over land is dominated by Africa (52 Gg-P yr^{-1}) and Asia (24 Gg-P yr^{-1}), both of which contain large areas of desert and reflect short-range transport from these important source regions. There is a considerable spatial variability over the ocean basins. The North Atlantic, North Pacific, and Indian Oceans dominate the absolute mass of Bio-P deposited to the surface waters accounting for 37%, 19%, and 18% of all Bio-P deposited to the oceans and seas, respectively. In the North Atlantic and Indian Ocean this is correlated with the dust mass deposition (52% and 21%), whilst the North Pacific accounts for only 11% of global dust supply to surface waters. This apparent enrichment is due to relatively enhanced acid dissolution, which will be discussed in the following section. The global importance of the Mediterranean Sea as a region impacted by dust is clearly demonstrated; it accounts for 5% of the total ocean Bio-P and results in the largest deposited mass per unit area over the oceans (1.5 µg-P $m^{-2}day^{-1}$) and is exceeded on land only by Africa (4.8 µg-P $m^{-2}day^{-1}$) and Asia (1.5 µg-P $m^{-2}day^{-1}$), which are both important dust source regions. The NE Atlantic is also strongly impacted because of its proximity to the Saharan

Desert, which exhibits a strong outflow over this region and results in a mean deposition rate of 1.2 μg-P $m^{-2}day^{-1}$.

3.2 Acid dissolution vs labile P

As observed by Stockdale et al. (2016) mineral dust contains Ap-P and Lab-P that both contribute towards the total fraction of inorganic mineral-borne phosphorus that is potentially bioavailable in marine surface waters. Although measurements reported by Stockdale et al. (2016) find Lab-P present in much smaller quantities than Ap-P, the total mass of Lab-P is directly bioavailable in the surface waters, whereas the Ap-P requires the presence of acid to yield a bioavailable form of P, hereafter referred to as Acid-P. The differences in immediate bioavailability of the two components results in distinct regional differences that can be seen in Figure 3 (panels a and b). Close to the dust source regions (Saharan, Arabian, Gobi, Patagonian, Kalahari, Great Basin, and Great Australian deserts) the Lab-P dominates the total Bio-P deposition, whereas further away from source regions and over industrialized regions Acid-P dominates; the formation of Acid-P is enhanced as dust accumulates condensed acids during long-range transport and when dust loading is low in proximity to local pollution sources (thus highlighting areas that are possibly acid-limited in respect to the dissolution of Ap-P). DMS can also play a role in providing a source of acid over the open oceans, especially in the Pacific Ocean, Southern Ocean, and Arctic Ocean (Belviso et al., 2004).

Table 1 and Table 2 provide regional information on the annual mean contribution from Lab-P and Acid-P. Of the total 31.2 Gg-P yr^{-1} of Bio-P deposited to the oceans 16.9 Gg-P yr^{-1} is from Acid-P and 14.3 Gg P yr^{-1} from Lab-P. The North Atlantic Ocean, Mediterranean Sea, and the western Indian Ocean, all regions strongly influenced by their proximity to significant dust sources, are dominated by the Lab-P fraction with 94% of the ocean's total Lab-P mass being deposited in these three regions (73%, 7%, and 14%, respectively). Conversely, the Pacific Ocean, Arctic Ocean, SE Atlantic, South China Sea, and the Southern Ocean, regions further from dust source regions, are dominated by the acid dissolution process; in these regions the contribution of Acid-P to the total Bio-P ranges from 75% to 81%. Although dominated by Lab-P the North Atlantic Ocean, Mediterranean Sea, and western Indian Ocean also receive a considerable mass of Bio-P from Acid-P. Considerable acid dissolution of Ap-P occurs over the Pacific Ocean even though this region receives a very small mass of dust (14% of global oceans dust supply, 25% of global oceans Bio-P supply).

3.3 Spatial variability of TP bioavailability

Estimated percentages of TP bioavailability for dust are shown in Figure 3c and Table 2. The simulated TP bioavailability from dust varies from ~10% to 60% and is generally negatively correlated with areas of high dust loading, and positively correlated with acid loading. The Lab-P content in dust tends to only vary between 9% and 11% of the TP across the globe (see Table 2). As this pool of phosphorus is deemed directly bioavailable, Bio-P in regions of high dust loading will be dominated by the Lab-P component and are likely to be less dependent on changes to acid concentrations. The dominance of Lab-P in high dust loading regions can be seen close to dust source regions over land and in the NE Atlantic Ocean where TP bioavailability (14%) is closely matched with the content of Lab-P in the dust (10%). Conversely, in regions that are not

dominated by dust loading, such as the central Pacific and the remote Arctic Ocean, Acid-P has a greater impact and results in a greater TP bioavailability (~50%). Due to the almost constant percentage of Lab-P in dust TP content the variability in TP bioavailability across the globe is controlled by the acid dissolution process; this is apparent from the wide range in percentage contribution of Acid-P in Table 2, which ranges from only 7% over Africa and 29% over the NE Atlantic, to over 77% in the Pacific and 81% over the Arctic Ocean. These findings highlight the importance that acid dissolution has on the deposition of Bio-P from dust to remote regions that have fewer sources of nutrients, such as the Greenland and Antarctic ice sheets, and the Arctic and Southern oceans. These estimates only refer to the bioavailability of dust-borne P. Results from the modelling study of Myriokefalitakis et al. (2016) suggest dust is the dominant driver of the collective bioavailability of P-containing aerosol species in northern hemisphere oceans, whereas in the southern hemisphere primary biological particles are more pronounced in the South Atlantic and South Pacific Oceans, and sea spray in the Southern Ocean. Therefore, our estimates are likely representative of northern hemisphere oceans, but other sources of P may increasingly drive the observed bioavailability in the high southern hemisphere latitudes.

3.4 Sensitivity of acid dissolution to degree of particle external mixing

The assumption used in this study is that a given mass of dust particles can be treated as if they are internally mixed, with each dust constituent (Ap-P, Lab-P, and $CaCO_3$) being present at a constant fraction of each particle's mass, i.e., in each grid box every particle will contain the same mass fraction of Ap-P, Lab-P, and $CaCO_3$. This is not necessarily important for the Lab-P fraction, but the dissolution of Ap-P into Acid-P occurs simultaneously with the dissolution of $CaCO_3$ at a rate that is faster than when no $CaCO_3$ is present.

To understand the importance of the particle mixing assumption, the deposited masses of dust and associated acid were split into distinct components to mimic a population of internally and externally mixed particles of varying concentrations. As previously, all Lab-P is deemed bioavailable, and hence the deposited Lab-P mass is the same as in the previous experiments. For a given percentage of externally mixed particles the relevant percentage mass of Ap-P is treated separately using Eq. 2 and assuming no $CaCO_3$ present, whilst the remaining mass of Ap-P is assumed internally mixed and treated as per the control experiment using Eq. 2 with the corresponding mass of $CaCO_3$. A third group, consisting of the externally mixed $CaCO_3$ is also removed but has no direct impact on the Bio-P and is simply removed along with its associated condensed acid (thereby having an indirect effect on Bio-P). The modelled uptake efficiency of acid onto the mineral particle is independent of the degree of external mixing. The total Bio-P deposited is the sum of Lab-P, internally mixed Acid-P, and externally mixed Acid-P. Externally mixed percentages of 1%, 2%, 5%, 10%, 25%, 50%, and an extreme case of 100% were used to determine the change in total Bio-P deposition to each region as a percentage of the control experiment where all particles are assumed to be internally mixed (0% externally mixed). Results are shown in Table 3.

The results show that the Bio-P deposition is very sensitive to the assumptions used for the distribution of components between dust particles. All regions show an increasing deposition rate of Bio-P with an increasing degree of external mixing. An increase from 0% to 5% results in a 9% increase of Bio-P to the oceans, with most of this from regions with large dust loadings

where acid dissolution of Ap-P is usually strongly buffered by $CaCO_3$. Regions that show less sensitivity are those where acid dissolution is already a dominating process and $CaCO_3$ is close to exhaustion; in this case the enhanced dissolution rate of Ap-P is already occurring. In reality it is unlikely that $CaCO_3$ and Ap-P will be exclusively present on different particles, but this provides insight of how sensitive the process is, and clearly suggests that this assumption is important for determining the dissolution process of Ap-P, and also other minerals that would usually be buffered by the $CaCO_3$.

3.5 Evaluation of model simulation

Our modelled deposition fluxes, solely from mineral dust, are evaluated against a dataset of observed fluxes and in-situ aerosol concentrations from ocean cruises and ground-based observations compiled by Vet et al. (2014) which includes data from a number of sources (Baker et al., 2006a; Baker et al., 2006b; Baker et al., 2010; Carbo et al., 2005; Chen and Chen, 2008; Chen, 2004; Furutani et al., 2010; Herut et al., 1999; Kocak et al., 2005; Koelliker et al., 2004; Markaki et al., 2003; Migon and Sandroni, 1999; Morales-Baquero et al., 2006; NADP/AIRMoN, 2010; Oredalen et al., 2010; Ozsoy, 2003; Rodríguez et al., 2011; Tamatamah et al., 2005; Zhang et al., 2007). Figure 4 and Figure 5a show the observations compared to the modelled deposition fluxes from our study. Although limited by observations, the model captures the regional variations in TP: the highest values are found close to source regions, such as the Mediterranean Sea and off the eastern coast of Africa, and lower values in more remote regions, such as the central Pacific. Apparently linear features in Figure 5a for the Pacific coast and Mediterranean occur due to multiple observations being present in the same model grid-box. Standard deviations of model data, shown in Figure 5a, show considerable variability throughout the year. The observational dataset contains P from all sources, whereas we only estimate fluxes for mineral dust. The results support the idea that mineral dust is a globally important source of P, but it is worth noting that in regions of low dust loading, such as the Southeast Pacific and Southern Ocean, other sources of P may play a more important role (Myriokefalitakis et al., 2016).

We also compared our Bio-P estimates to field observations in Figure 4 and Figure 5b. The model reproduces the observations within an order magnitude for much of the Atlantic Ocean and Mediterranean Sea but, as with TP, is under-estimating values over the Pacific Ocean and the land; the under-representation over land is likely due to the enhanced role of other sources of P. A key result is that when acid dissolution is removed from the model, shown in Figure 5b using crossed symbols, the Bio-P values are systematically too low compared with measurements. The normalized mean bias (and with respect to the logarithm) without acid dissolution is -0.60 (-0.27) and -0.54 (-0.1) when acid dissolution is included. Our model confirms that acid dissolution in the atmosphere is an important process affecting the deposited flux of Bio-P (through the addition of Acid-P) to the Earth's surface.

Overall TP deposition fluxes to ocean basins and seas are compared to other modelling studies in Table 4. Regional trends show good agreement with other studies: The North Atlantic Ocean is the globally dominant region for deposition, with the North Pacific Ocean and Indian Ocean also important regions for deposition. Our results show good agreement with Zhang et al. (2013), who similarly only considered mineral dust, in all regions except for the North Atlantic for which

the authors estimate an additional 40% deposition of TP. Okin et al. (2011) and Myriokefalitakis et al. (2016) estimate similar fluxes for the Atlantic Ocean but estimate a factor of ~2 to 3 greater deposition to the Pacific and Indian oceans. Mahowald et al. (2008) estimate considerably greater fluxes in most regions: the Atlantic Ocean is a factor of 3 greater, and the Pacific and Indian oceans are a factor of ~4 greater than our estimates. These differences are largely due to the assumed P content of dust. In our study the P content of the emitted dust was determined using a soil P-content database from Yang et al. (2013), which results in a global mean TP content of 489 ppm per mass of dust. Mahowald et al. (2008), assumed a constant P content of 720 ppm, Okin et al. (2011) use 700 ppm, whilst Myriokefalitakis et al. (2016) use a soil database (Nickovic et al., 2012) and tune emissions to result in a global mean dust TP content of 880 ppm. Using these alternative global mean contents and our modelled dust fluxes would result in equivalent ocean TP deposition fluxes of 212, 206, and 259 Gg-P yr^{-1}.

Table 4 also compares Bio-P from this study with other modelling studies. Zhang et al. (2015) provide a good comparison as their study only considers inorganic P from dust and uses a globally constant TP bioavailability for each mineral, experimentally determined in solution with a pH of 2. In contrast we use a parameterization based on experiments using a full range of conditions, which results in a TP bioavailability that depends on acidity levels and dust loading. In Zhang et al. (2015) the TP bioavailability is ~10% for most of the basins, whereas in this study the bioavailability varies from ~15% in areas of high dust loading to > 45% in regions of high pollution or remote regions only accessible through long-range transport. This results in a global deposition of Bio-P in our study (31.2 Gg-P yr^{-1}) that is roughly double that of Zhang et al. (2015). Mahowald et al. (2008) estimate Bio-P ocean deposition of 96.5 Gg-P yr^{-1}, which is roughly three times our estimate. In their study a constant TP bioavailability of 10% for mineral dust is used, However, the inclusion of other P sources results in a TP bioavailability from all P sources that is greater than 10% in regions where other P sources are important, such as the Pacific and Arctic. The increased TP from other sources, and from the assumed TP content of dust, results in a greater Bio-P deposition estimate than our study.

Myriokefalitakis et al. (2016) estimate 88.7 Gg-P yr^{-1} Bio-P from inorganic sources only (dust-borne Lab-P, dissolved Ap-P, and volcanic aerosols), which is a factor of ~3 greater than our study; this difference arises mainly through differences in the TP content of dust, as well as a different modelled acid dissolution process, and through contributions from volcanic aerosols (6 Gg-P yr^{-1} predominantly to the Pacific Ocean). If we apply the higher dust TP and Lab-P content from Myriokefalitakis et al. (2016), it increases our global Bio-P estimate by 16 Gg-P yr^{-1}. The final difference occurs through the treatment of the Acid-P production; we estimate 30 Gg-P yr^{-1} is deposited globally as Acid-P, compared to 144 Gg-P yr^{-1} by Myriokefalitakis et al. (2016). Part of this difference in Acid-P is due to the assumption used in Myriokefalitakis et al. (2016) that the TP content of dust is comprised of Lab-P and Ap-P only, whereas other constituents are included in our soil database (e.g., Lab-P and Ap-P make up ~50% of TP in the Sahara Desert). Assuming our deposited dust is only comprised of Lab-P and Ap-P would provide a factor 3 increase in Ap-P availability, which as shown by our sensitivity study (Table S2) could have a considerable impact on Bio-P deposition. The final differences in Acid-P production occur in the different representations of acid dissolution: in our study the empirically parameterized process is dependent on the absolute number of H^+ ions from H_2SO_4 and HNO_3 uptake and calculated offline after deposition, whereas in Myriokefalitakis et al.

(2016) an online aerosol thermodynamic equilibrium framework is used to determine conditions for use in a kinetic model. The added sources of atmospheric acid and detailed treatment of the particle's aqueous composition results in greater acid dissolution than the simple experimentally based method used in our study. However, despite these differences it is an interesting result that the two methods produce similar spatial patterns but of different magnitudes. Assessing these differences and identifying the more appropriate method are beyond the scope of this study but merit further attention.

4 Discussion

There is large spatial variability in the amount of Bio-P supplied to the surface ocean. The largest flux of dust and of Bio-P, predominantly in the form of Lab-P, is supplied to the NE Atlantic Ocean; this area is known to have a high dust flux from the world's major source of mineral dust, the Sahara Desert. The modelling suggests that this area not only has the highest total input of Bio-P (6.9 Gg-P yr^{-1}) but also a high input of Bio-P per unit area (436 µg-P $m^{-2}yr^{-1}$; second to the Mediterranean Sea with 549 µg-P $m^{-2}yr^{-1}$). Neuer et al. (2004) suggest the pulses of Saharan dust seem to exert a feast or famine effect on phytoplankton export from this region. A pulsing that may be linked to the observed phytoplankton export is apparent in the modelled fluxes (Figures S3 to S6) which vary between 0.2 and 0.6 Gg-P per month in the NE Atlantic and between 0.4 and 0.9 Gg-P per month in the NW Atlantic, another region with considerable deposition of Bio-P. In these regions, Saharan dust plumes transported over the N Atlantic meet N American air masses which are enriched in anthropogenic combustion products. Sedwick et al. (2007) identified an increase in soluble Fe delivered to the offshore NW Atlantic caused by the N American polluted air masses. Here we show based on our modelling that these air masses also increase the amount of Acid-P from the mineral dust transported across the Atlantic from the Sahara, especially during the summer months when dust transport and acid pollution are both relatively enhanced.

The total Bio-P supplied to the ocean is the sum of contributions from Lab-P and Acid-P. The location with the highest mass of deposited Bio-P from Acid-P is the NW Pacific (3.6 Gg-P yr^{-1}). Our data (Table 1) is averaged over the whole NW Pacific area, however the impact is greatest in the area directly under the plume from the Gobi and Taklamakan deserts which passes over the highly polluted air in East Asia (Jaffe et al., 1999) and out into the NW Pacific (Chen et al., 2017). This plume is rather narrowly confined to ~40°N but has a large effect within that plume as shown in Figures S3 and S4. We see the strongest peak during the Northern Hemisphere spring (March-April-May; Figure S5), which is consistent with the findings of Chen et al. (2017). Maki et al. (2016) find that Asian dust is a major nutrient source to the area of the NW Pacific under the plume though their study concentrates on the flux of atmospheric nitrate to this N limited region. As argued below the greatly increased flux of Bio-P from the dust plume will reduce the potential effect of switching to P limitation and may also increase the N_2 fixation in the surface waters (Jickells and Moore, 2015) as well as increasing the total primary productivity over longer timescales (Tyrell, 1999).

The location with the highest annual mass of Bio-P per unit area (~550 µg-P $m^{-2}yr^{-1}$) is the Mediterranean Sea. This area is particularly sensitive to the addition of extra Bio-P since both the Western and particularly the Eastern Mediterranean are P limited (Krom et al., 1991; Moutin and

Raimbault, 2002; Powley et al., 2017). Any addition of P available to the phytoplankton will rapidly be taken up into the P-starved water (Krom et al., 2005) and be translated into extra primary productivity. Microcosm experiments have shown the importance of dust inputs to increasing primary productivity particularly during the summer when there is minimal nutrient supply from below (Laghdass et al., 2012; Ridame et al., 2014). Krom et al. (2010) estimated that Lab-P from atmospheric sources provided 30% of the non-marine external P supplied to the Eastern Mediterranean while Powley et al. (2017), using a mass-balance model, estimated that 49% of the non-marine external supply to the entire Mediterranean was from atmospheric supply. African dust outbreaks are estimated by Pey et al. (2013) to occur over the Mediterranean over 20% of annual days. These plumes of mineral dust, along with locally derived sources, meet air polluted with acidic gases from Europe including air that has passed over cities such as Athens (Nenes et al., 2011); this results in extra Acid-P, and thus Bio-P, being produced. The modelling results are compatible with the predictions made by Nenes et al. (2011) concerning the effect of acid processing on mineral aerosol over the Mediterranean.

There is also a considerable contribution from Acid-P in both the western and eastern Indian Ocean. This is an area where dust from local desert regions such as the Arabian Peninsula and the Thar desert in India meet with air masses polluted from highly populated areas in South and South-East Asia (Lelieveld et al., 2001), and pollution from biomass burning over Central and South-eastern Africa and South Asia (Sinha et al., 2004). It has been suggested that atmospheric aerosols including dust particles, as well as biomass burning and other anthropogenic sources, are increasing the flux of dissolved nutrients (including phosphate) to the Bay of Bengal (Srinivas and Sarin, 2015). Rengarajan and Sarin (2004) suggested that aerosols that have been involved in interactions between mineral dust and pollution also impacted the Arabian Sea; they identified its effect on Fe and NOx. Here we suggest it also affects the Acid-P.

It is generally assumed that any potential Bio-P (i.e., mineral apatite and/or Fe-bound P) as well as Lab-P that lands on most parts of the terrestrial system will be consumed by plants. Plants and their accompanying mycorrhizal fungi are evolved to extract this key nutrient from such minerals present in the soil (Smits et al., 2012). The only exception to this might be areas of snow, such as Greenland and the Arctic, which host algal communities which are important for climate change due to their impact on surface albedo (Lutz et al., 2016). It has been reported that microbes in arctic glaciers live in P-deficient environments (Stibal et al., 2009) which suggests that atmospheric input of Bio-P to these key regions may play an important role on local algal and microbial activity. We estimate that the amount of Bio-P delivered to the major ice sheets of the world (Greenland and Antarctica) is 0.08 Gg-P yr^{-1} of which the majority (~80%) is produced by acid dissolution.

Modelling studies routinely use a constant value for TP bioavailability, which typically ranges from ~10 to ~15%. From the soil P database used in our study we show that TP bioavailability is at least 10% due to Lab-P alone and is considerably greater once the Acid-P contribution is included. For inorganic Bio-P from mineral dust we estimate global mean TP bioavailability of 22% and 12% for oceans and land, respectively. For the ocean basins, we estimate the following: Pacific Ocean (425%); Atlantic Ocean (18%); Indian Ocean (20%); Mediterranean (15%); Southern Ocean (46%); and Arctic Ocean (55%). Other studies such as Myriokefalitakis et al. (2016) show similar increases in TP bioavailability caused by Acid-P. These calculations suggest

that while the spatial variability of TP and Bio-P are similar (Table 4), the absolute fluxes vary considerably to a large extent because of different values for TP in the source material. Uncertainties in current soil databases primarily arise from a lack of observations and sampling of under-represented soil types, including species that contain phosphorus (Nickovic et al., 2012; Yang et al., 2013); the result is poor spatial coverage and a lack of process-level understanding that yields considerable uncertainties. The sensitivity experiments (Table 3 and Table S2) highlight the clear need for improved estimates of dust-borne P components at source.

Krishnamurthy et al. (2010) calculated that the addition of atmospheric P to the global ocean will increase the total carbon uptake by 0.12% based on an estimated 8.3 Gg-P yr^{-1} Bio-P deposited to the oceans. However, the authors assumed a globally constant dust TP content of 1050 ppm and a globally constant TP bioavailability of 15%. In comparison our model estimates Bio-P deposition from inorganic mineral dust to be ~400% of this value (31.2 Gg-P yr^{-1}) with TP bioavailability ranging from ~15% to ~50%. Our enhanced Bio-P deposition estimate suggests the total carbon uptake could be even greater, if the apatite and $CaCO_3$ composition in the mineral dust population were externally mixed. Assuming all Bio-P is taken up by phytoplankton, and applying the Redfield ratio, our results suggest the atmospheric input of Bio-P from mineral dust may account for an uptake of 1.3 Tg-C yr^{-1}, with 0.7 Tg-C yr^{-1} from acid-dissolution of mineral dust. If the mineral dust Ap-P/$CaCO_3$ content is deemed 100% externally mixed, then the total uptake would be 3.0 Tg-C yr^{-1}.

In non Fe-limited areas where the system is N limited in the short term, it has been shown that most atmospheric input has a high bioavailable N:P ratio and an excess of Fe. It has been suggested that the input of Fe and N causes the systems to switch towards P limitation (Jickells and Moore, 2015). The increased Bio-P shown to be formed by these atmospheric acid processes linked mainly to anthropogenic pollution will slow this process down particularly in areas like the NW Atlantic (Chien et al., 2016). This study suggests that the abundant acid gases produced during volcanic eruptions are likely to have a short term but possibly dramatic effect on the supply of Bio-P to the ocean. Previous work has been confined to the actual Bio-P produced within the volcanic plume itself, which is rather small (e.g., Mahowald et al., 2008). Here we predict that a more important effect might be to increase the flux of Bio-P to the ocean due to the interaction of acid gasses from the volcano with existing mineral particles in the atmosphere.

Stoichiometric proxies have been used to estimate nitrogen fixation rates in oceanic surface waters. Deutsch et al., (2007) calculated a parameter ($P^* = PO_4^{3-} - NO_3^-/16$) and suggested that regions with high P* are also regions of the ocean with high N_2 fixation rates and vice versa. It is noticeable that the three regions of the global ocean with low values of P* in their calculations (north central Atlantic, north western Pacific, and Mediterranean) are also the areas with the predicted highest fluxes of Acid-P. Superficially the addition of extra bio-P should increase P*, however a large fraction of the acid which produces acid-P is nitric acid. This is apparent in the Eastern Mediterranean where the Atmospheric N:P ratio has been observed as high as 105:1 (Markaki et al., 2010). This is an area of the ocean with very low N_2 fixation rates (Yogev et al., 2011). By contrast the N_2 fixation rate of the north central Atlantic is relatively high because the high flux of Saharan dust contains abundant Fe and P, which are required by N_2 fixing organisms (Mills et al., 2004). It is unclear what overall impact the external supply of bio-P from mineral

dust has on N_2 fixation rates and P*, however, our results provide global estimates that may help to improve our understanding in the future.

5 Summary

In this study a parameterization for acid-dissolution of mineral apatite, developed using results presented by Stockdale et al. (2016), was incorporated into a global aerosol model (GLOMAP; Mann et al., 2010) with a global soil P database (Yang et al., 2013) to model the atmospheric flux of inorganic bioavailable P from mineral dust. We estimate that 870 G-P yr^{-1} of inorganic TP associated with dust is deposited globally, with 726 Gg-P yr^{-1} to the land and 144 Gg-P yr^{-1} to the oceans. Our model is able to discriminate between the leachable (labile) pool of phosphorus which is present upon emission and the dissolved apatite pool which is a result of the simultaneous acid-dissolution of apatite and calcium-carbonate; the two pools combined represent the atmospheric flux of bioavailable phosphorus from dust.

We estimate a global flux of 31 Gg-P yr^{-1} Bio-P to the oceans with 14.3 Gg-P yr^{-1} from the labile pool (Lab-P), and 16.9 Gg-P yr^{-1} from the acid-dissolved pool (Acid-P). The acid dissolution of mineral dust increases supply of Bio-P to the oceans by 120%, showing the importance of the acid dissolution process on global Bio-P fluxes. We identify the Mediterranean Sea, North Atlantic Ocean, and North Pacific Ocean as particularly important regions for dust-borne Bio-P deposition.

Our modelling results show that the percentage of deposited dust TP that is in a bioavailable form ranges from ~10% to ~50%, however, generally it has been assumed in modelling studies that the percentage of mineral dust TP bioavailability is globally constant, with values between 10% and 15% commonly used. We use a similar approach to Myriokefalitakis et al. (2016) to show that although the labile fraction of TP is globally constant at ~10%, the acid-dissolved pool increased the mean TP bioavailability over oceans to 22% with considerable variation between ocean basins: Pacific Ocean (45%); Atlantic Ocean (23%); Indian Ocean (21%); and Mediterranean (15%). This variability again highlights the impact that the acid-dissolution process has on the global flux of Bio-P from dust.

The world's largest dust sources all have relatively enriched levels of dust-P pools but show variability between sources. We therefore advise against using global constant values for dust-P pools and recommend using global databases of soil-P content. In our study we used a pedogenesis-based soil-P database from Yang et al. (2013) which resulted in a global mean deposited dust TP content of 489 ppm with 49 ppm from Lab-P and 243 ppm from Ap-P, with all pools displaying roughly one order of magnitude variability across the globe. Comparing these results with other modelling studies and results from a series of sensitivity tests highlighted the affect that the assumed dust mineralogical content has on the Bio-P flux. It is noted that there is no consensus on the global mean deposited dust TP and previous studies have used higher values (e.g., 880 ppm by Myriokefalitakis et al. (2016) and 720 ppm by Mahowald et al. (2008)). From our sensitivity study we have identified that treating the dust population as an externally rather than internally mixed population (i.e., assuming the population exhibits particle-to-particle diversity in apatite and $CaCO_3$ content) results in a considerable increase in global Bio-P flux (44% increase for a 25% externally mixed population). It is currently not known which treatment is appropriate and requires more research.

Our results confirm the importance of acid processes in the atmosphere in increasing the flux of Bio-P to the global ocean as suggested by Nenes et al. (2011). The effect is spatially and temporally variable and it is suggested that increased Bio-P can result in regionally important changes in biogeochemical processes such as nutrient limitation, nitrogen fixation rates and carbon uptake.

Acknowledgements

This research was funded by the Leverhulme Trust Research Project Grant RPG 406, entitled "Understanding the Delivery of phosphorus nutrient to the oceans". KSC acknowledges funding from the EU CRESCENDO project under grant agreement No 641816. The authors wish to thank T. Nenes, M. Kanikidou, and S. Myriokefalitakis for useful discussions and for providing data used in the comparison to Myriokefalitakis et al. (2016). The authors also wish to thank R. Vet for providing the observational dataset used; this source is listed in the references. Other data used are listed in the references, tables, and supplementary information.

References

Atkinson, J. D., Murray, B. J., Woodhouse, M. T., Whale, T. F., Baustian, K. J., Carslaw, K. S., Dobbie, S., O'Sullivan, D., and Malkin, T. L. (2013), The importance of feldspar for ice nucleation by mineral dust in mixed-phase clouds. *Nature*, 498, 355-358. 10.1038/nature12278

Baker, A. R., French, M., and Linge, K. L. (2006a), Trends in aerosol nutrient solubility along a west–east transect of the Saharan dust plume. *Geophysical Research Letters*, 33, L07805. 10.1029/2005gl024764

Baker, A. R., Jickells, T. D., Witt, M., and Linge, K. L. (2006b), Trends in the solubility of iron, aluminium, manganese and phosphorus in aerosol collected over the Atlantic Ocean. *Marine Chemistry*, 98, 43-58. 10.1016/j.marchem.2005.06.004

Baker, A. R., Lesworth, T., Adams, C., Jickells, T. D., and Ganzeveld, L. (2010), Estimation of atmospheric nutrient inputs to the Atlantic Ocean from 50°N to 50°S based on large-scale field sampling: Fixed nitrogen and dry deposition of phosphorus. *Global Biogeochemical Cycles*, 24, GB3006. 10.1029/2009gb003634

Belviso, S., Moulin, C., Bopp, L., and Stefels, J. (2004), Assessment of a global climatology of oceanic dimethylsulfide (DMS) concentrations based on SeaWiFS imagery (1998-2001). *Canadian Journal of Fisheries and Aquatic Sciences*, 61, 804-816. 10.1139/f04-001

Brahney, J., Mahowald, N., Ward, D. S., Ballantyne, A. P., and Neff, J. C. (2015), Is atmospheric phosphorus pollution altering global alpine Lake stoichiometry? *Global Biogeochemical Cycles*, 29, 1369-1383. 10.1002/2015gb005137

Browse, J., Carslaw, K. S., Arnold, S. R., Pringle, K., and Boucher, O. (2012), The scavenging processes controlling the seasonal cycle in Arctic sulfate and black carbon aerosol. *Atmospheric Chemistry and Physics*, 12, 6775-6798. 10.5194/acp-12-6775-2012

Carbo, P., Krom, M. D., Homoky, W. B., Benning, L. G., and Herut, B. (2005), Impact of atmospheric deposition on N and P geochemistry in the southeastern Levantine basin. *Deep Sea Research Part II: Topical Studies in Oceanography*, 52, 3041-3053. 10.1016/j.dsr2.2005.08.014

Chen, H.-Y., & Chen, L.-D. (2008), Importance of anthropogenic inputs and continental-derived dust for the distribution and flux of water-soluble nitrogen and phosphorus species in aerosol within the atmosphere over the East China Sea. *Journal of Geophysical Research*, 113, D11303. 10.1029/2007jd009491

Chen, S., Huang, J., Kang, L., Wang, H., Ma, X., He, Y., Yuan, T., Yang, B., Huang, Z., and Zhang, G. (2017), Emission, transport, and radiative effects of mineral dust from the Taklimakan and Gobi deserts: comparison of measurements and model results. *Atmospheric Chemistry and Physics*, 17, 2401-2421. 10.5194/acp-17-2401-2017

Chen, Y. (2004), Sources and Fate of Atmospheric Nutrients over the Remote Oceans and Their Role on Controlling Marine Diazotrophic Microorganisms, Ph.D. diss., Univ. of Maryland, College Park.

Chien, C.-T., Mackey, K. R. M., Dutkiewicz, S., Mahowald, N. M., Prospero, J. M., and Paytan, A. (2016), Effects of African dust deposition on phytoplankton in the western tropical Atlantic Ocean off Barbados. *Global Biogeochemical Cycles*, 30, 716-734. 10.1002/2015gb005334

Chipperfield, M. P. (2006), New version of the TOMCAT/SLIMCAT off-line chemical transport model: Intercomparison of stratospheric tracer experiments. *Quarterly Journal of the Royal Meteorological Society*, 132, 1179-1203. 10.1256/qj.05.51

Dentener, F., Kinne, S., Bond, T., Boucher, O., Cofala, J., Generoso, S., Ginoux, P., Gong, S., Hoelzemann, J. J., Ito, A., Marelli, L., Penner, J. E., Putaud, J. P., Textor, C., Schulz, M., van der Werf, G. R., and Wilson, J. (2006), Emissions of primary aerosol and precursor gases in the years 2000 and 1750 prescribed data-sets for AeroCom. *Atmospheric Chemistry and Physics*, 6, 4321-4344. 10.5194/acp-6-4321-2006

Deutsch, C., Sarmiento, J. L., Sigman, D. M., Gruber, N., Dunne, J. P. (2007), Spatial coupling of nitrogen inputs and losses in the ocean. *Nature*, 445, 163-167. 10.1038/nature05392

Diehl, T., Heil, A., Chin, M., Pan, X., Streets, D., Schultz, M., and Kinne, S. (2012), Anthropogenic, biomass burning, and volcanic emissions of black carbon, organic carbon, and SO_2 from 1980 to 2010 for hindcast model experiments. *Atmospheric Chemistry and Physics Discussions*, 12, 24895-24954. 10.5194/acpd-12-24895-2012

Eijsink, L. M., Krom, M. D., and Herut, B. (2000), Speciation and burial flux of phosphorus in the surface sediments of the eastern Mediterranean. *American Journal of Science*, 300, 483-503. 10.2475/ajs.300.6.483

Fuchs, N. A., and Sutugin, A. G. (1971), High-Dispersed Aerosols, in: Topics in Current Aerosol Research, edited by: Brock, J. R., Pergamon, 1.

Furutani, H., Meguro, A., Iguchi, H., and Uematsu, M. (2010), Geographical distribution and sources of phosphorus in atmospheric aerosol over the North Pacific Ocean. *Geophysical Research Letters*, 37, L03805. 10.1029/2009gl041367

Graham, W. F., and Duce, R. A. (1967), The atmospheric transport of phosphorus to the western North Atlantic. *Atmospheric Environment*, 16, 1089-1097. 10.1016/0004-6981(82)90198-6

Herut, B., Krom, M. D., Pan, G., and Mortimer, R. (1999), Atmospheric input of nitrogen and phosphorus to the Southeast Mediterranean: Sources, fluxes, and possible impact. *Limnology and Oceanography*, 44, 1683-1692. 10.4319/lo.1999.44.7.1683

Herut, B., Zohary, T., Krom, M. D., Mantoura, R. F. C., Pitta, P., Psarra, S., Rassoulzadegan, F., Tanaka, T., and Frede Thingstad, T. (2005), Response of East Mediterranean surface water to Saharan dust: On-board microcosm experiment and field observations. *Deep Sea Research Part II: Topical Studies in Oceanography*, 52, 3024-3040. 10.1016/j.dsr2.2005.09.003

Huneeus, N., Schulz, M., Balkanski, Y., Griesfeller, J., Prospero, J., Kinne, S., Bauer, S., Boucher, O., Chin, M., Dentener, F., Diehl, T., Easter, R., Fillmore, D., Ghan, S., Ginoux, P., Grini, A., Horowitz, L., Koch, D., Krol, M. C., Landing, W., Liu, X., Mahowald, N., Miller, R., Morcrette, J. J., Myhre, G., Penner, J., Perlwitz, J., Stier, P., Takemura, T., and Zender, C. S. (2011), Global dust model intercomparison in AeroCom phase I. *Atmospheric Chemistry and Physics*, 11, 7781-7816. 10.5194/acp-11-7781-2011

Jaffe, D., Anderson, T., Covert, D., Kotchenruther, R., Trost, B., Danielson, J., Simpson, W., Berntsen, T., Karlsdottir, S., Blake, D., Harris, J., Carmichael, G., and Uno, I. (1999), Transport of Asian air pollution to North America. *Geophysical Research Letters*, 26, 711-714. 10.1029/1999GL900100

Jickells, T., and Moore, C. M. (2015), The Importance of Atmospheric Deposition for Ocean Productivity. *Annual Review of Ecology, Evolution, and Systematics*, 46, 481-501. 10.1146/annurev-ecolsys-112414-054118

Kanakidou, M., Duce, R. A., Prospero, J. M., Baker, A. R., Benitez-Nelson, C., Dentener, F. J., Hunter, K. A., Liss, P. S., Mahowald, N., Okin, G. S., Sarin, M., Tsigaridis, K., Uematsu, M., Zamora, L. M., and Zhu, T. (2012), Atmospheric fluxes of organic N and P to the global ocean. *Global Biogeochemical Cycles*, 26, GB3026. 10.1029/2011gb004277

Kettle, A. J., Andreae, M. O., Amouroux, D., Andreae, T. W., Bates, T. S., Berresheim, H., Bingemer, H., Boniforti, R., Curran, M. A. J., DiTullio, G. R., Helas, G., Jones, G. B., Keller, M.

D., Kiene, R. P., Leck, C., Levasseur, M., Malin, G., Maspero, M., Matrai, P., McTaggart, A. R., Mihalopoulos, N., Nguyen, B. C., N 258ovo, A., Putaud, J. P., Rapsomanikis, S., Roberts, G., Schebeske, G., Sharma, S., Simó, R., Staubes, R., Turner, S., and Uher, G. (1999), A global database of sea surface dimethylsulfide (DMS) measurements and a procedure to predict sea surface DMS as a function of latitude, longitude, and month. *Global Biogeochemical Cycles*, 13, 399-444. 10.1029/1999gb900004

Kocak, M., Kubilay, N., Herut, B., and Nimmo, M. (2005), Dry atmospheric fluxes of trace metals (Al, Fe, Mn, Pb, Cd, Zn, Cu) over the Levantine Basin: A refined assessment. *Atmospheric Environment*, 39, 7330-7341. 10.1016/j.atmosenv.2005.09.010

Koelliker, Y., Totten, L. A., Gigliotti, C. L., Offenberg, J. H., Reinfelder, J. R., Zhuang, Y., and Eisenreich, S. J. (2004), Atmospheric Wet Deposition of Total Phosphorus in New Jersey. *Water, Air, & Soil Pollution*, 154, 139-150. 10.1023/B:WATE.0000022952.12577.c5

Krishnamurthy, A., Moore, J. K., Mahowald, N., Luo, C., and Zender, C. S. (2010), Impacts of atmospheric nutrient inputs on marine biogeochemistry. *Journal of Geophysical Research*, 115, G01006. 10.1029/2009jg001115

Krom, M. D., Kress, N., Brenner, S., and Gordon, L. I. (1991), Phosphorus limitation of primary productivity in the eastern Mediterranean Sea. *Limnology and Oceanography*, 36, 424-432. 10.4319/lo.1991.36.3.0424

Krom, M. D., Thingstad, T. F., Brenner, S., Carbo, P., Drakopoulos, P., Fileman, T. W., Flaten, G. A. F., Groom, S., Herut, B., Kitidis, V., Kress, N., Law, C. S., Liddicoat, M. I., Mantoura, R. F. C., Pasternak, A., Pitta, P., Polychronaki, T., Psarra, S., Rassoulzadegan, F., Skjoldal, E. F., Spyres, G., Tanaka, T., Tselepides, A., Wassmann, P., Wexels Riser, C., Woodward, E. M. S., Zodiatis, G., and Zohary, T. (2005), Summary and overview of the CYCLOPS P addition Lagrangian experiment in the Eastern Mediterranean. *Deep Sea Research Part II: Topical Studies in Oceanography*, 52, 3090-3108. 10.1016/j.dsr2.2005.08.018

Krom, M. D., Emeis, K. C., and Van Cappellen, P. (2010), Why is the Eastern Mediterranean phosphorus limited? *Progress in Oceanography*, 85, 236-244. 10.1016/j.pocean.2010.03.003

Laghdass, M., Catala, P., Caparros, J., Oriol, L., Lebaron, P., and Obernosterer, I. (2012), High contribution of SAR11 to microbial activity in the north west Mediterranean Sea. *Microb Ecol*, 63, 324-333. 10.1007/s00248-011-9915-7

Lelieveld, J., Crutzen, P. J., Ramanathan, V., Andreae, M. O., Brenninkmeijer, C. A. M., Campos, T., Cass, G. R., Dickerson, R. R., Fischer, H., de Gouw, J. A., Hansel, A., Jefferson, A., Kley, D., de Laat, A. T. J., Lal, S., Lawrence, M. G., Lobert, J. M., Mayol-Bracero, O. L., Mitra, A. P., Novakov, T., Oltmans, S. J., Prather, K. A., Reiner, T., Rodhe, H., Scheeren, H. A., Sikka, D., and Williams, J. (2001), The Indian Ocean Experiment: Widespread Air Pollution from South and Southeast Asia. *Science*, 291, 1031-1036. 10.1126/science.1057103

Lutz, S., Anesio, A. M., Raiswell, R., Edwards, A., Newton, R. J., Gill, F., and Benning, L. G. (2016), The biogeography of red snow microbiomes and their role in melting arctic glaciers. *Nature Comms*, 7, 11968. 10.1038/ncomms11968

Mahowald, N., Jickells, T. D., Baker, A. R., Artaxo, P., Benitez-Nelson, C. R., Bergametti, G., Bond, T. C., Chen, Y., Cohen, D. D., Herut, B., Kubilay, N., Losno, R., Luo, C., Maenhaut, W., McGee, K. A., Okin, G. S., Siefert, R. L., and Tsukuda, S. (2008), Global distribution of atmospheric phosphorus sources, concentrations and deposition rates, and anthropogenic impacts. *Global Biogeochemical Cycles*, 22, GB4026. 10.1029/2008gb003240

Mahowald, N. M. (2004), Comment on "Relative importance of climate and land use in determining present and future global soil dust emission" by I. Tegen et al. *Geophysical Research Letters*, 31, L24105. 10.1029/2004gl021272

Maki, T., Ishikawa, A., Mastunaga, T., Pointing, S. B., Saito, Y., Kasai, T., Watanabe, K., Aoki, K., Horiuchi, A., Lee, K. C., Hasegawa, H., Iwasaka, Y. (2016), Atmospheric aerosol deposition influences marine microbial communities in oligotrophic surface waters of the western Pacific Ocean. *Deep-Sea Research*, 118, 37-45. 10.1016/j.dsr.2016.10.002

Mann, G. W., Carslaw, K. S., Spracklen, D. V., Ridley, D. A., Manktelow, P. T., Chipperfield, M. P., Pickering, S. J., and Johnson, C. E. (2010), Description and evaluation of GLOMAP-mode: a modal global aerosol microphysics model for the UKCA composition-climate model. *Geoscientific Model Development*, 3, 519-551. 10.5194/gmd-3-519-2010

Markaki, Z., Oikonomou, K., Kocak, M., Kouvarakis, G., Chaniotaki, A., Kubilay, N., and Mihalopoulos, N. (2003), Atmospheric deposition of inorganic phosphorus in the Levantine Basin, eastern Mediterranean: Spatial and temporal variability and its role in seawater productivity. *Limnology and Oceanography*, 48, 1557-1568. 10.4319/lo.2003.48.4.1557

Markaki, Z., Loÿe-Pilot, M. D., Violaki, K., Benyahya, L., Mihalopoulos, N. (2010), Variability of atmospheric deposition of dissolved nitrogen and phosphorus in the Mediterranean and possible link to the anomalous seawater N/P ratio. *Marine Chemistry*, 120, 187-194. 10.1016/j.marchem.2008.10.005

Migon, C., & Sandroni, V. (1999), Phosphorus in rainwater: Partitioning inputs and impact on the surface coastal ocean. *Limnology and Oceanography*, 44, 1160-1165. 10.4319/lo.1999.44.4.1160

Mills, M. M., Ridame, C., Davey, M., La Roche, J., Geider, R. J. (2004), Iron and phosphorus co-limit nitrogen fixation in the eastern tropical North Atlantic. *Nature*, 429, 292-294. 10.1038/nature02550

Morales-Baquero, R., Pulido-Villena, E., and Reche, I. (2006), Atmospheric inputs of phosphorus and nitrogen to the southwest Mediterranean region: Biogeochemical responses of high mountain lakes. *Limnology and Oceanography*, 51, 830-837. 10.4319/lo.2006.51.2.0830

Moutin, T., & Raimbault, P. (2002), Primary production, carbon export and nutrients availability in western and eastern Mediterranean Sea in early summer 1996 (MINOS cruise). *Journal of Marine Systems*, 33-34, 273-288. 10.1016/S0924-7963(02)00062-3

Myriokefalitakis, S., Nenes, A., Baker, A. R. (2016), Mihalopoulos, N., and Kanakidou, M.: Bioavailable atmospheric phosphorous supply to the global ocean: a 3-D global modeling study. *Biogeosciences*, 13, 6519-6543. 10.5194/bg-13-6519-2016

NADP/AIRMoN: (Atmospheric Integrated Research Monitoring Network), (2010), National Atmospheric Deposition Program (NADP) Office, Illinois State Water Survey, 2204 Griffith Dr., Champaign, IL, U.S., Website: http://nadp.sws.uiuc.edu/AIRMoN/

Nenes, A., Krom, M. D., Mihalopoulos, N., Van Cappellen, P., Shi, Z., Bougiatioti, A., Zarmpas, P., and Herut, B. (2011), Atmospheric acidification of mineral aerosols: a source of bioavailable phosphorus for the oceans. *Atmospheric Chemistry and Physics*, 11, 6265-6272. 10.5194/acp-11-6265-2011

Neuer, S., Torres-Padrón, M. E., Gelado-Caballero, M. D., Rueda, M. J., Hernández-Brito, J., Davenport, R., and Wefer, G. (2004), Dust deposition pulses to the eastern subtropical North Atlantic gyre: Does ocean's biogeochemistry respond? *Global Biogeochemical Cycles*, 18, GB4020. 10.1029/2004gb002228

Nickovic, S., Vukovic, A., Vujadinovic, M., Djurdjevic, V., and Pejanovic, G. (2012), Technical Note: High-resolution mineralogical database of dust-productive soils for atmospheric dust modeling. *Atmospheric Chemistry and Physics*, 12, 845-855. 10.5194/acp-12-845-2012

Nightingale, P. D., Malin, G., Law, C. S., Watson, A. J., Liss, P. S., Liddicoat, M. I., Boutin, J., and Upstill-Goddard, R. C. (2000), In situ evaluation of air-sea gas exchange parameterizations using novel conservative and volatile tracers. *Global Biogeochemical Cycles*, 14, 373-387. 10.1029/1999gb900091

Okin, G. S., Baker, A. R., Tegen, I., Mahowald, N. M., Dentener, F. J., Duce, R. A., Galloway, J. N., Hunter, K., Kanakidou, M., Kubilay, N., Prospero, J. M., Sarin, M., Surapipith, V., Uematsu, M., and Zhu, T. (2011), Impacts of atmospheric nutrient deposition on marine productivity: Roles of nitrogen, phosphorus, and iron. *Global Biogeochemical Cycles*, 25, GB2022. 10.1029/2010gb003858

Oredalen, T., Aas, W., and Maenhaut, W. (2010), Atmospheric dry and wet deposition of phosphorus in southern Norway. In: *Data obtained from the World Meteorological Organization Scientific Advisory Group of Precipitation Chemistry Workshop*, Berg-en-Dal, South Africa, 15-20 March 2010

Ozsoy, T. (2003), Atmospheric wet deposition of soluble macro-nutrients in the Cilician Basin, north-eastern Mediterranean sea. *J Environ Monit*, 5, 971-976. 10.1039/B309636J

Parkhurst, D. L., & Appelo, C. A. J. (2013), Description of input and examples for PHREEQC version 3 - A computer program for speciation, batch-reaction, one-dimensional transport, and inverse geochemical calculations. *U.S. Geological Survey Techniques and Methods*, Book 6

Pey, J., Querol, X., Alastuey, A., Forastiere, F., and Stafoggia, M. (2013), African dust outbreaks over the Mediterranean Basin during 2001-2011: PM_{10} concentrations, phenomenology and trends, and its relation with synoptic and mesoscale meteorology. *Atmospheric Chemistry and Physics*, 13, 1395-1410. 10.5194/acp-13-1395-2013

Powley, H. R., Krom, M. D., and Van Cappellen, P. (2017), Understanding the unique biogeochemistry of the Mediterranean Sea: Insights from a coupled phosphorus and nitrogen model. *Global Biogeochemical Cycles*, 31, 1010-1031. 10.1002/2017gb005648

Rengarajan, R., and Sarin, M. M. (2004), Atmospheric deposition fluxes of 7Be, 210Pb and chemical species to the Arabian Sea and Bay of Bengal. *Indian Journal of Marine Sciences*, 33, 56-64.

Ridame, C., Dekaezemacker, J., Guieu, C., Bonnet, S., L'Helguen, S., and Malien, F. (2014), Contrasted Saharan dust events in LNLC environments: impact on nutrient dynamics and primary production. *Biogeosciences*, 11, 4783-4800. 10.5194/bg-11-4783-2014

Rodríguez, S., Alastuey, A., Alonso-Pérez, S., Querol, X., Cuevas, E., Abreu-Afonso, J., Viana, M., Pérez, N., Pandolfi, M., and de la Rosa, J. (2011), Transport of desert dust mixed with North African industrial pollutants in the subtropical Saharan Air Layer. *Atmospheric Chemistry and Physics*, 11, 6663-6685. 10.5194/acp-11-6663-2011

Ruttenberg, K. C. (2003), The Global Phosphorus Cycle. *Treatise on Geochemistry*, 8, 585-643. 10.1016/B0-08-043751-6/08153-6

Sedwick, P. N., Sholkovitz, E. R., and Church, T. M. (2007), Impact of anthropogenic combustion emissions on the fractional solubility of aerosol iron: Evidence from the Sargasso Sea. *Geochemistry, Geophysics, Geosystems*, 8, Q10Q06. 10.1029/2007gc001586

Shangguan, W., Dai, Y., Duan, Q., Liu, B., and Yuan, H. (2014), A global soil data set for earth system modeling. *Journal of Advances in Modeling Earth Systems*, 6, 249-263. 10.1002/2013ms000293

Sinha, P., Jaeglé, L., Hobbs, P. V., and Liang, Q. (2004), Transport of biomass burning emissions from southern Africa. *Journal of Geophysical Research: Atmospheres*, 109, D20204. 10.1029/2004JD005044

Slinn, W. G. N. (1982), Predictions for particle deposition to vegetative canopies. *Atmospheric Environment*, 16, 1785-1794. 10.1016/0004-6981(82)90271-2

Smits, M. M., Bonneville, S., Benning, L. G., Banwart, S. A., Leake, J. R. (2012), Plant-driven weathering of apatite – the role of an ectomycorrhizal fungus. *Geobiology*, 10, 445-456. 10.1111/j.1472-4669.2012.00331.x

Srinivas, B., & Sarin, M. M. (2015), Atmospheric deposition of phosphorus to the Northern Indian Ocean. *Current Science*, 108, 1300-1305. 10.1016/j.scitotenv.2013.03.068

Stibal, M., Anesio, A. M., Blues, C. J. D., Tranter, M. (2009), Phosphatase activity and organic phosphorus turnover on a high Arctic glacier. *Biogeosciences*, 6, 913-922. 10.5194/bg-6-913-2009

Stockdale, A., Krom, M. D., Mortimer, R. J., Benning, L. G., Carslaw, K. S., Herbert, R. J., Shi, Z., Myriokefalitakis, S., Kanakidou, M., and Nenes, A. (2016), Understanding the nature of atmospheric acid processing of mineral dusts in supplying bioavailable phosphorus to the oceans. *Proc Natl Acad Sci USA*, 113, 14639-14644. 10.1073/pnas.1608136113

Tamatamah, R. A., Hecky, R. E., and Duthie, H. (2005), The atmospheric deposition of phosphorus in Lake Victoria (East Africa). *Biogeochemistry*, 73, 325-344. 10.1007/s10533-004-0196-9

Thingstad, T. F., Krom, M. D., Mantoura, R. F., Flaten, G. A., Groom, S., Herut, B., Kress, N., Law, C. S., Pasternak, A., Pitta, P., Psarra, S., Rassoulzadegan, F., Tanaka, T., Tselepides, A., Wassmann, P., Woodward, E. M., Riser, C. W., Zodiatis, G., and Zohary, T. (2005), Nature of phosphorus limitation in the ultraoligotrophic eastern Mediterranean. *Science*, 309, 1068-1071. 10.1126/science.1112632

Tipping, E., Benham, S., Boyle, J. F., Crow, P., Davies, J., Fischer, U., Guyatt, H., Helliwell, R., Jackson-Blake, L., Lawlor, A. J., Monteith, D. T., Rowe, E. C., and Toberman, H. (2014), Atmospheric deposition of phosphorus to land and freshwater. *Environ Sci Process Impacts*, 16, 1608-1617. 10.1039/c3em00641g

Tyrrell, T. (1999), The relative influences of nitrogen and phosphorus on oceanic primary production. *Nature*, 400, 525-531. 10.1038/22941

van der Werf, G. R., Randerson, J. T., Giglio, L., Collatz, G. J., Mu, M., Kasibhatla, P. S., Morton, D. C., DeFries, R. S., Jin, Y., and van Leeuwen, T. T. (2010), Global fire emissions and the contribution of deforestation, savanna, forest, agricultural, and peat fires (1997–2009). *Atmospheric Chemistry and Physics*, 10, 11707-11735. 10.5194/acp-10-11707-2010

Vergara-Temprado, J., Murray, B. J., Wilson, T. W., amp, apos, Sullivan, D., Browse, J., Pringle, K. J., Ardon-Dryer, K., Bertram, A. K., Burrows, S. M., Ceburnis, D., DeMott, P. J., Mason, R. H., amp, apos, Dowd, C. D., Rinaldi, M., and Carslaw, K. S. (2017), Contribution of feldspar and marine organic aerosols to global ice nucleating particle concentrations. *Atmospheric Chemistry and Physics*, 17, 3637-3658. 10.5194/acp-17-3637-2017

Vet, R., Artz, R. S., Carou, S., Shaw, M., Ro, C.-U., Aas, W., Baker, A., Bowersox, V. C., Dentener, F., Galy-Lacaux, C., Hou, A., Pienaar, J. J., Gillett, R., Forti, M. C., Gromov, S., Hara, H., Khodzher, T., Mahowald, N. M., Nickovic, S., Rao, P. S. P., and Reid, N. W. (2014), A global assessment of precipitation chemistry and deposition of sulfur, nitrogen, sea salt, base cations, organic acids, acidity and pH, and phosphorus. *Atmospheric Environment*, 93, 3-100. 10.1016/j.atmosenv.2013.10.060

Wang, R., Balkanski, Y., Bopp, L., Aumont, O., Boucher, O., Ciais, P., Gehlen, M., Penuelas, J., Ethe, C., Hauglustaine, D., Li, B., Liu, J., Zhou, F., and Tao, S. (2015), Influence of anthropogenic aerosol deposition on the relationship between oceanic productivity and warming. *Geophys Res Lett*, 42, 10745-10754. 10.1002/2015GL066753

Wu, J., Sunda, W., Boyle, E. A., and Karl, D. M. (2000), Phosphate depletion in the western North Atlantic Ocean. *Science*, 289, 759-762. 10.1126/science.289.5480.759

Yang, X., Post, W. M., Thornton, P. E., and Jain, A. (2013), The distribution of soil phosphorus for global biogeochemical modeling. *Biogeosciences*, 10, 2525-2537. 10.5194/bg-10-2525-2013

Yogev, T., Rahav, E., Bar-Zeev, E., Man-Aharonovich, D., Stambler, N., Kress, N., Béjà, O., Mulholland, M. R., Herut, B., Berman-Frank, I. (2011), Is dinitrogen fixation significant in the Levantine Basin, East Mediterranean Sea? *Environmental Microbiology*, 13, 854-871. doi:10.1111/j.1462-2920.2010.02402.x

Zamora, L. M., Prospero, J. M., Hansell, D. A., and Trapp, J. M. (2013), Atmospheric P deposition to the subtropical North Atlantic: sources, properties, and relationship to N deposition. *Journal of Geophysical Research: Atmospheres*, 118, 1546-1562. 10.1002/jgrd.50187

Zhang, G., Zhang, J., and Liu, S. (2007), Characterization of nutrients in the atmospheric wet and dry deposition observed at the two monitoring sites over Yellow Sea and East China Sea. *Journal of Atmospheric Chemistry*, 57, 41-57. 10.1007/s10874-007-9060-3

Zhang, Y., Mahowald, N., Scanza, R. A., Journet, E., Desboeufs, K., Albani, S., Kok, J. F., Zhuang, G., Chen, Y., Cohen, D. D., Paytan, A., Patey, M. D., Achterberg, E. P., Engelbrecht, J. P., and Fomba, K. W. (2015), Modeling the global emission, transport and deposition of trace elements associated with mineral dust. *Biogeosciences*, 12, 5771-5792. 10.5194/bg-12-5771-2015

Tables

Table 1. Absolute mass of bioavailable phosphorus (total and from each source) and dust components deposited to the surface of each region in the simulated year. All units are in Gg-P yr^{-1} except for dust which is in Tg yr^{-1}. Values in parentheses give annual mass per unit area in µg-P $m^{-2}yr^{-1}$ except for dust which is in mg $m^{-2}yr^{-1}$.

Region		Bioavailable phosphorus deposition			Deposited dust content	
		Total (Bio-P)	from acid dissolution (Acid-P)	from labile pool (Lab-P)	Total phosphorus (TP)	Total dust *
Ice sheets						
Greenland		0.03 (18)	0.03 (15)	0.01 (3)	0.06 (30)	0.11 (57)
Antarctic		0.05 (3)	0.04 (3)	0.01 (1)	0.09 (6)	0.12 (8)
Oceans and Seas						
Arctic Ocean		0.5 (36)	0.4 (29)	0.1 (7)	0.9 (66)	1.7 (123)
Pacific Ocean	NE	2.5 (66)	1.8 (51)	0.5 (15)	5.2 (147)	10.7 (303)
	SE	0.8 (14)	0.6 (11)	0.1 (3)	1.5 (26)	3.0 (53)
	NW	3.6 (87)	2.7 (65)	0.9 (22)	9.5 (230)	22.1 (535)
	SW	1.2 (38)	0.9 (30)	0.2 (8)	2.6 (86)	5.9 (192)
Atlantic Ocean	NE	6.9 (436)	2.0 (125)	4.9 (310)	48.4 (3041)	103.4 (6497)
	SE	2.1 (70)	1.6 (52)	0.5 (18)	5.5 (184)	10.9 (360)
	NW	4.7 (181)	2.2 (84)	2.5 (98)	24.5 (943)	50.8 (1959)
	SW	1.1 (95)	0.6 (56)	0.4 (39)	4.9 (431)	7.8 (689)
Baltic Sea		0.05 (146)	0.03 (105)	0.01 (40)	0.13 (391)	0.23 (689)
Mediterranean Sea		1.5 (549)	0.5 (177)	1.0 (372)	9.8 (3592)	16.3 (5962)
Indian Ocean	W	3.5 (89)	1.5 (39)	2.0 (50)	20.2 (516)	42.0 (1074)
	E	2.2 (62)	1.4 (39)	0.8 (23)	8.7 (245)	19.7 (559)
South China Sea		0.5 (68)	0.4 (54)	0.1 (14)	1.2 (148)	2.7 (327)
Southern Ocean		0.3 (14)	0.2 (11)	0.1 (3)	0.6 (31)	1.0 (53)
Continents						
Europe		3.5 (364)	1.9 (199)	1.6 (165)	15.4 (1612)	26.9 (2822)
North America		2.0 (87)	1.4 (62)	0.6 (25)	6.1 (270)	10.9 (483)
South America		3.3 (180)	1.4 (79)	1.8 (101)	19.4 (1074)	32.3 (1793)
Africa		51.6 (1738)	3.5 (119)	48.1 (1619)	466.8 (15725)	940.4 (31681)
Asia		23.6 (562)	4.6 (109)	19.0 (453)	198.5 (4725)	425.8 (10138)
Australia		2.3 (282)	0.5 (65)	1.7 (218)	19.9 (2480)	44.5 (5555)
Antarctica		0.05 (3)	0.04 (3)	0.01 (1)	0.09 (6)	0.12 (8)
Totals						
Global total		117 (229)	30 (59)	87 (170)	870 (1695)	1779 (3468)
Ocean total		31.2 (84)	16.9 (45)	14.3 (39)	144 (392)	298 (814)
Land total		86 (595)	13 (92)	73 (503)	726 (5013)	1481 (10225)

all units in Gg-P yr^{-1} (µg-P $m^{-2}yr^{-1}$)
* dust in Tg yr^{-1} (mg $m^{-2}yr^{-1}$)

Table 2. Annual means: percentage of total-P in deposited dust bioavailable at surface; percentage of bioavailable-P from acid dissolution of apatite; percentage of total-P in dust from labile-P; and percentage of apatite-P in deposited dust dissolved by acid dissolution.

Region		% of TP in dust bioavailable at surface	% of bio-P from acid dissolution	% of TP in dust from labile pool	% of Ap-P in dust dissolved
Ice sheets					
Greenland		62 %	82 %	11 %	100 %
Antarctic		60 %	82 %	11 %	93 %
Oceans and Seas					
Arctic Ocean		55 %	81 %	10 %	86 %
Pacific Ocean	NE	45 %	77 %	10 %	73 %
	SE	52 %	81 %	10 %	84 %
	NW	38 %	75 %	10 %	56 %
	SW	44 %	80 %	9 %	65 %
Atlantic Ocean	NE	14 %	29 %	10 %	9 %
	SE	38 %	75 %	10 %	58 %
	NW	19 %	46 %	10 %	19 %
	SW	22 %	59 %	9 %	28 %
Baltic Sea		37 %	72 %	10 %	54 %
Mediterranean Sea		15 %	32 %	10 %	10 %
Indian Ocean	W	17 %	43 %	10 %	14 %
	E	25 %	63 %	9 %	31 %
South China Sea		46 %	79 %	10 %	70 %
Southern Ocean		45 %	79 %	10 %	74 %
Continents					
Europe		23 %	55 %	10 %	25 %
North America		32 %	71 %	9 %	45 %
South America		17 %	44 %	9 %	16 %
Africa		11 %	7 %	10 %	12 %
Asia		12 %	19 %	10 %	4 %
Australia		11 %	23 %	9 %	5 %
Antarctica		60 %	82 %	11 %	93 %
Global means					
Global mean		14 %	26 %	10 %	7 %
Ocean mean		22 %	54 %	10 %	24 %
Land mean		12 %	16 %	10 %	4 %

Table 3. Sensitivity of annual deposited mass of bioavailable phosphorus to degree of external mixing of apatite and calcium carbonate ($CaCO_3$) content in the deposited dust. Data show percentage increase of bioavailable phosphorus compared to the control run (0% mixing; internally mixed assumption). An externally mixed percentage of 0% implies that apatite and dust are present at the same ratio in all dust particles (therefore internally mixed) and a percentage of 100% implies that apatite and calcium carbonate are exclusively present in different dust particles.

		Percentage of apatite and $CaCO_3$ externally mixed in dust						
Region		1%	2%	5%	10%	25%	50%	100%
Ice sheets								
Greenland		0	0	0	0	0	0	0
Antarctic		0	0	0	1	2	4	5
Oceans and Seas								
Arctic		0	0	1	2	4	7	11
Pacific	NE	0	1	2	4	9	17	24
	SE	0	0	1	2	4	8	12
	NW	1	1	4	7	17	33	48
	SW	1	1	3	5	12	24	34
Atlantic	NE	3	6	15	31	77	153	229
	SE	1	1	3	6	15	29	43
	NW	2	4	10	20	51	102	152
	SW	2	3	8	16	39	78	116
Baltic		1	1	3	7	17	33	49
Mediterranean		3	6	15	29	73	148	221
Indian	W	3	5	13	26	66	132	198
	E	1	3	7	15	37	74	110
South China		0	1	2	4	9	19	27
Southern		0	1	2	3	8	16	23
Ocean total		2	4	9	18	44	88	131

all data in % increase compared to control run

Table 4. Modelled deposition fluxes of TP and Bio-P to different ocean basins in Gg-P yr^{-1}. Figures in parentheses correspond to the TP bioavailability (%) upon deposition. Bio-P data from Zhang et al. (2015) are presented for their 'sol-1' dataset (please refer to the study for details). Values for both total dissolved phosphorus (DP) and dissolved inorganic phosphorus (DIP) from Myriokefalitakis et al. (2016) are included. Values from Zhang et al. (2015) and this study are only for phosphorus from inorganic mineral dust.

	Mahowald et al. 2008		Okin et al. 2011		Zhang et al. 2015*		Myriokefalitakis et al. 2016			This study*	
	TP	Bio-P	TP	Bio-P	TP	Bio-P sol-1	TP	Bio-P DP	Bio-P DIP †	TP	Bio-P
Atlantic	**232**	35.8 (15)	**128**	-	**112**	9.6 (9)	**110**	54.9 (50)	36.6	**83**	14.8 (18)
N Atlantic	**190**	27.9 (15)	-	-	**103**	8.8 (9)	**96**	44.2 (46)	32.3	**73**	11.6 (16)
S Atlantic	**42**	7.9 (19)	-	-	**9**	0.8 (9)	**14**	10.6 (74)	4.4	**10**	3.2 (30)
Pacific	**85**	28 (33)	**68**	-	**18**	1.8 (9)	**60**	48.4 (81)	26.6	**20**	8.4 (42)
N Pacific	**63**	22 (35)	-	-	**18**	1.7 (10)	**47**	38.0 (80)	23.9	**15**	5.9 (40)
S Pacific	**22**	6 (27)	-	-	**1**	0.07 (8)	**12**	10.5 (86)	2.7	**5**	2.5 (47)
Indian	**149**	20.3 (14)	**73**	-	**37**	3.8 (10)	**56**	37.3 (66)	20.7	**29**	5.7 (20)
Southern	**12**	1.7 (14)	**32**	-	**0.2**	0.01 (7)	**2**	1.5 (82)	0.2	**1**	0.5 (46)
Arctic	**7**	2.2 (32)	-	-	**1**	0.1 (10)	**5**	3.3 (74)	1.7	**1**	0.5 (55)
Mediterranean	**54**	5.7 (11)	-	-	**11**	1.1 (10)	**7**	4.4 (59)	2.7	**10**	1.5 (15)
Antarctic ice	-	-	-	-	**0.1**	0.01 (9)	**0.1**	0.0 (23)	0.0	**0.1**	0.1 (60)
Greenland ice	-	-	-	-	**5**	0.5 (9)	**0.3**	0.2 (62)	0.1	**0.1**	0.03 (62)
Ocean total	**558**	96.5 (17)	**320**	-	**180**	16.3 (9)	**240**	150.2 (63)	88.7	**144**	31.2 (22)
Land total	**831**	143.5 (17)	-	-	-	-	**1051**	303 (29)	160	**726**	86 (12)

* mineral dust only

† dissolved inorganic P from dust and volcanic emissions only

Figures

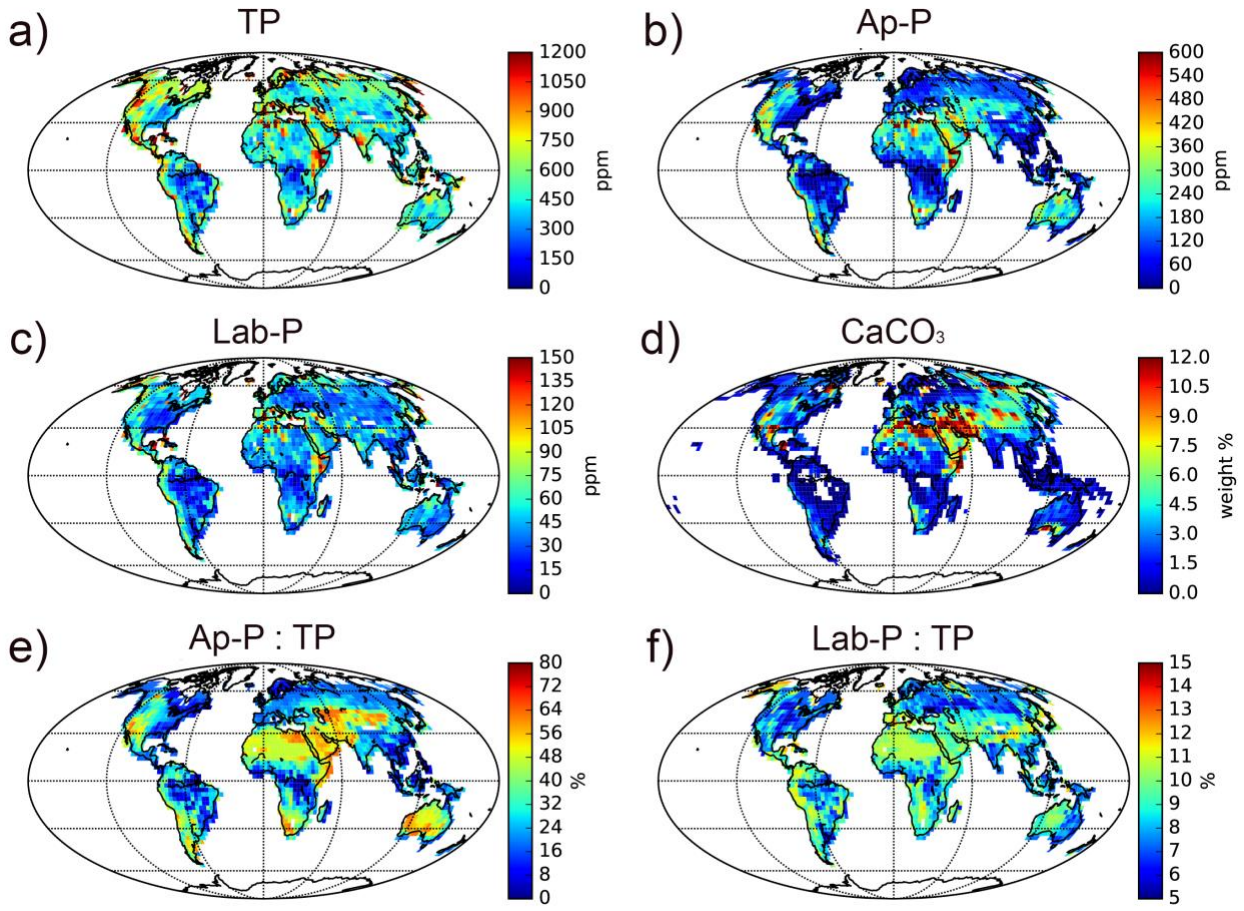

Figure 1. Global gridded datasets used for GLOMAP dust-associated emissions of **a)** total-phosphorus (ppm); **b)** apatite-phosphorus (ppm); **c)** labile-phosphorus (ppm); **d)** calcium-carbonate (%); **e)** ratio of apatite-phosphorus to total-phosphorus (%); and **f)** ratio of labile-phosphorus to total-phosphorus (%).

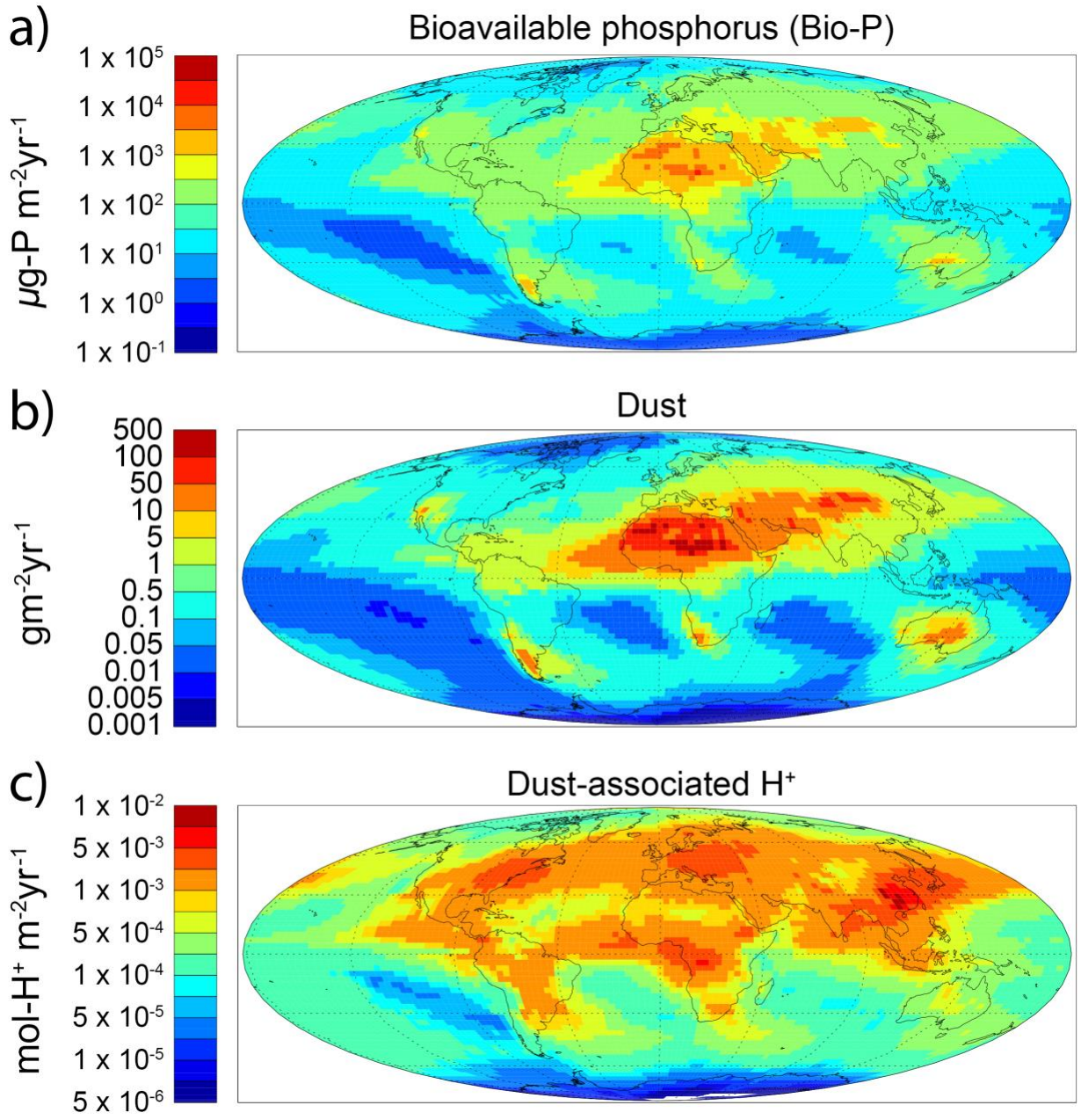

Figure 2. Annual deposition rate of **a)** bioavailable phosphorus in µg-P $m^{-2}yr^{-1}$, **b)** dust in g $m^{-2}yr^{-1}$, and **c)** dust-associated H^+ ions in mol-H^+ $m^{-2}yr^{-1}$.

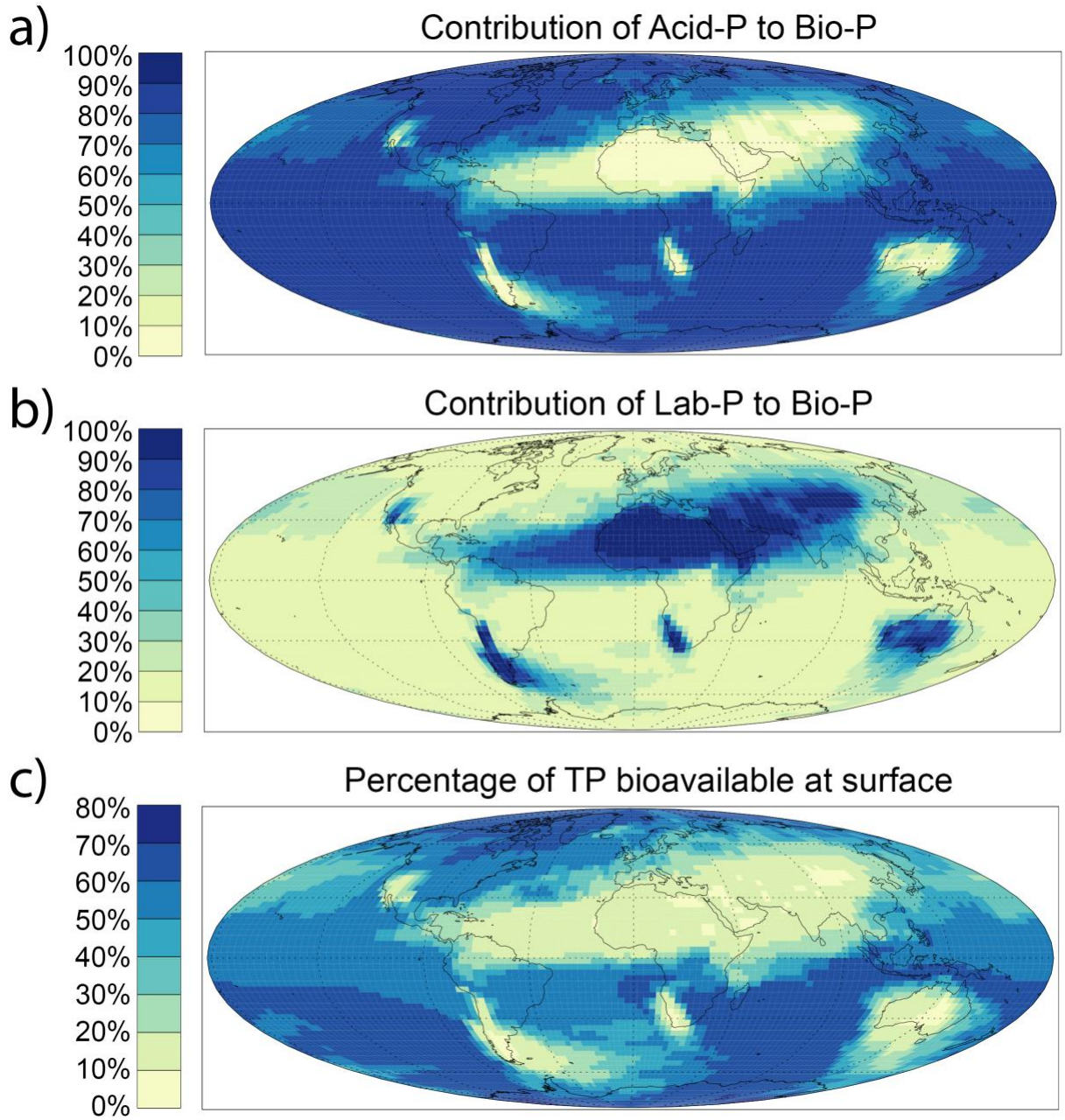

Figure 3. Annual mean percentage contribution of **a)** the acid dissolution process and **b)** the labile pool of phosphorus to the total bioavailable phosphorus from dust deposition, and **c)** the percentage of the total phosphorus content in dust that is bioavailable upon deposition.

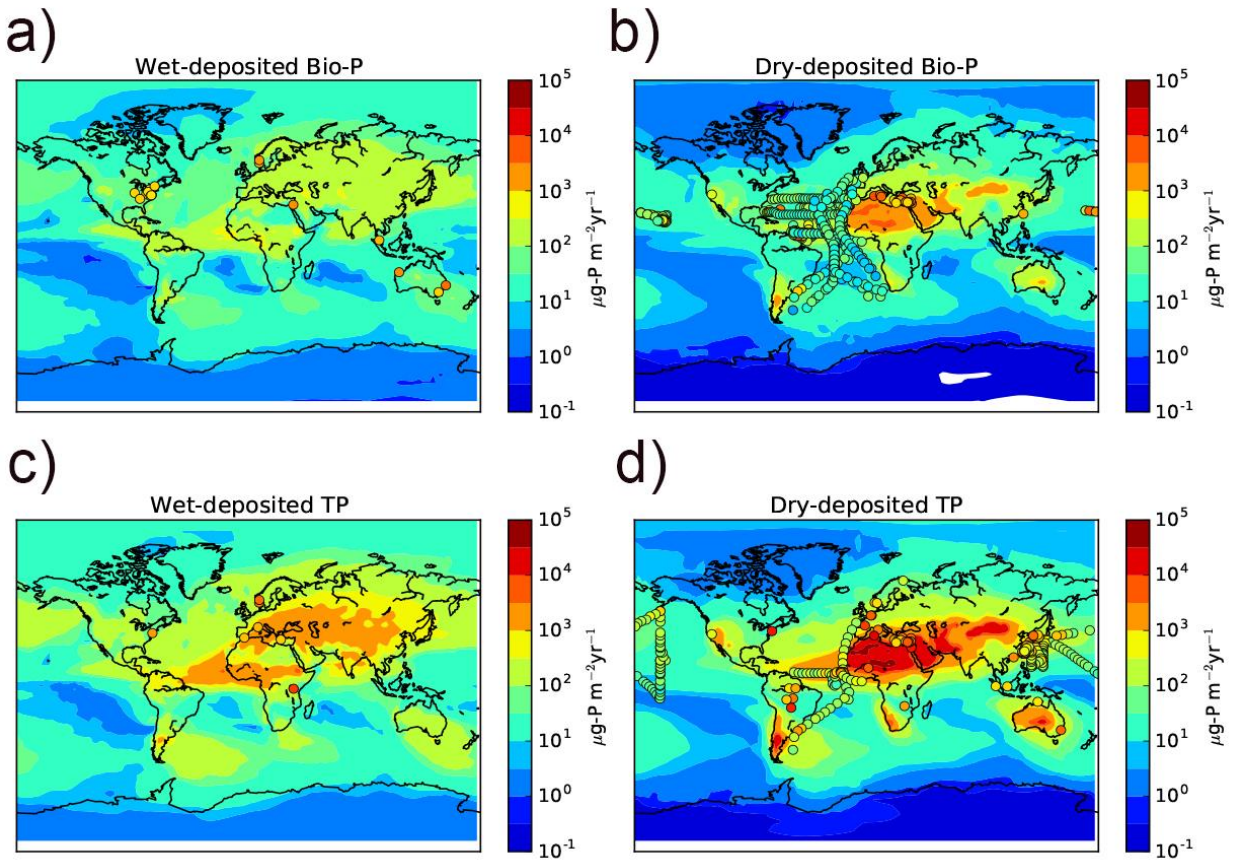

Figure 4. Modelled deposition fluxes (contours) and observations (filled circles) from Vet et al. (2014) in µg-P $m^{-2}yr^{-1}$ for **a)** wet-deposited TP, **b)** dry-deposited TP, **c)** wet-deposited Bio-P, and **d)** dry-deposited Bio-P. Modelled and observational values follow the same color scale.

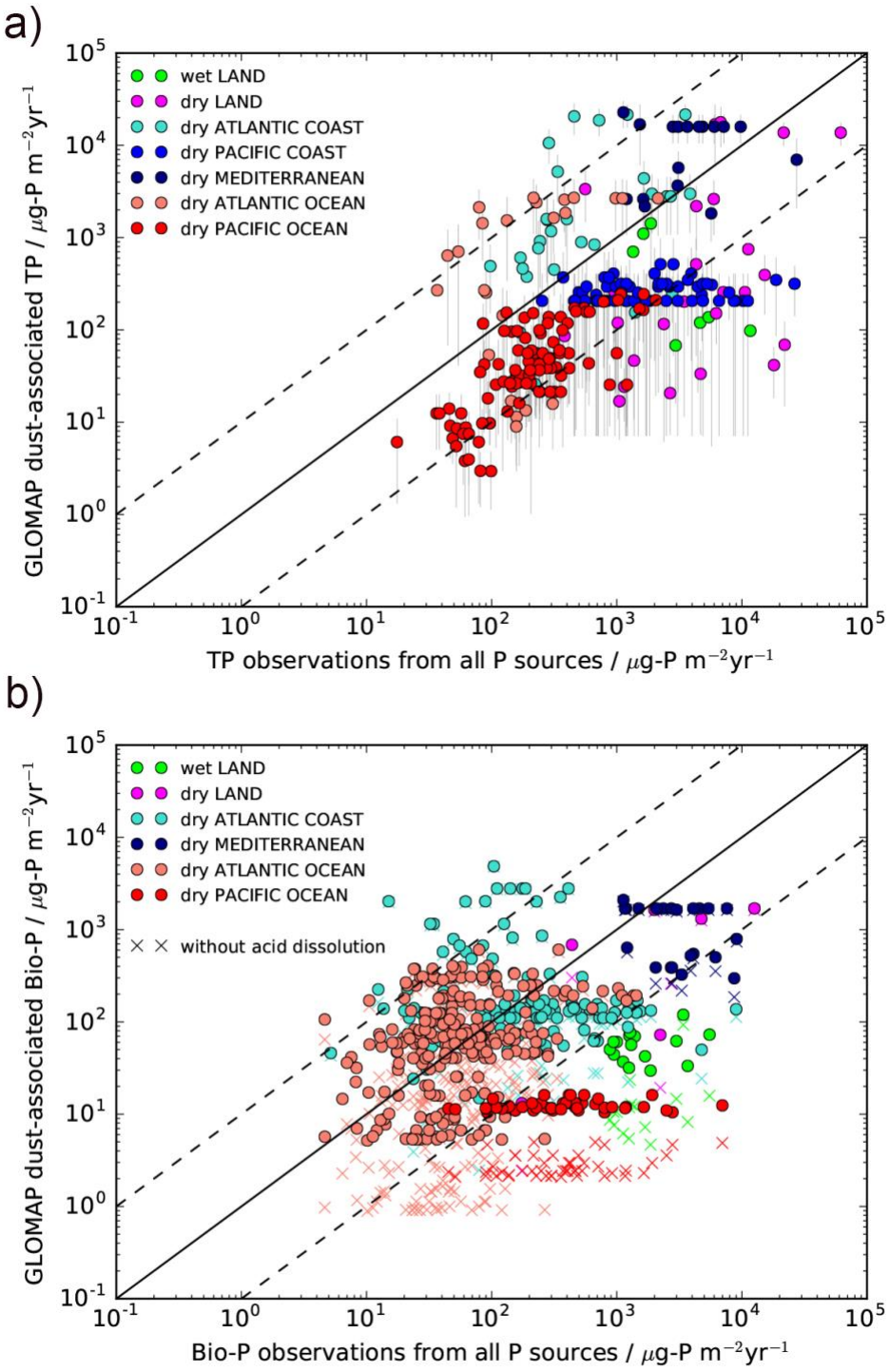

Figure 5. Data as in Figure 4 but shown as scatter plots with observations from Vet et al. (2014) on the x-axis and modelled fluxes from this study on the y-axis. **a)** shows data for TP fluxes and **b)** for Bio-P fluxes. Different colored circles depict different regions. Vertical lines in a) show the standard deviation of modelled deposition flux at that location from the simulated year (not repeated in b) for clarity). Crosses in b) show the modelled deposition flux of Bio-P without simulated acid dissolution of apatite.